Calcium phosphate nanoparticles as intrinsic inorganic antimicrobials: In search of the key particle property

Vuk Uskoković, Sean Tang, Marko G. Nikolić, Smilja Marković, and Victoria M. Wu

Citation: Biointerphases **14**, 031001 (2019); doi: 10.1116/1.5090396
View online: https://doi.org/10.1116/1.5090396
View Table of Contents: https://avs.scitation.org/toc/bip/14/3
Published by the American Vacuum Society

Calcium phosphate nanoparticles as intrinsic inorganic antimicrobials: In search of the key particle property

Vuk Uskoković,[1,2] Sean Tang,[2] Marko G. Nikolić,[3] Smilja Marković,[4] and Victoria M. Wu[2]
[1]*Department of Bioengineering, University of Illinois, Chicago, Illinois 60607-7052*
[2]*Advanced Materials and Nanobiotechnology Laboratory, Department of Biomedical and Pharmaceutical Sciences, Center for Targeted Drug Delivery, Chapman University, Irvine, California 92618-1908*
[3]*Institute of Physics, University of Belgrade, Pregrevica 118, 11080 Belgrade, Serbia*
[4]*Institute of Technical Sciences of the Serbian Academy of Sciences and Arts (SASA), Knez Mihailova 35/IV, 11000 Belgrade, Serbia*

(Received 27 January 2019; accepted 6 May 2019; published 20 May 2019)

One of the main goals of materials science in the 21st century is the development of materials with rationally designed properties as substitutes for traditional pharmacotherapies. At the same time, there is a lack of understanding of the exact material properties that induce therapeutic effects in biological systems, which limits their rational optimization for the related medical applications. This study sets the foundation for a general approach for elucidating nanoparticle properties as determinants of antibacterial activity, with a particular focus on calcium phosphate nanoparticles. To that end, nine physicochemical effects were studied and a number of them were refuted, thus putting an end to frequently erred hypotheses in the literature. Rather than having one key particle property responsible for eliciting the antibacterial effect, a complex synergy of factors is shown to be at work, including (a) nanoscopic size; (b) elevated intracellular free calcium levels due to nanoparticle solubility; (c) diffusivity and favorable electrostatic properties of the nanoparticle surface, primarily low net charge and high charge density; and (d) the dynamics of perpetual exchange of ultrafine clusters across the particle/solution interface. On the positive side, this multifaceted mechanism is less prone to induce bacterial resistance to the therapy and can be a gateway to the sphere of personalized medicine. On a more problematic side, it implies a less intense effect compared to single-target molecular therapies and a difficulty of elucidating the exact mechanisms of action, while also making the rational design of theirs for this type of medical application a challenge. *Published by the AVS.* https://doi.org/10.1116/1.5090396

I. INTRODUCTION

The unceasing coevolution of the microbiota and complex organisms requires constant innovation in the domain of strategies and forms by which pathological bacterial growths are kept in check. One of the essential goals for biomaterials science in the new millennium is to discover materials that could either replace the traditional, small-molecule antibiotics or act in synergy that boosts the activity of weak or ineffective antibiotics. Traditional antibiotics are notorious for their promotion of microbial resistance, low targeting potential, and an array of systemic side effects, which are all issues amendable with the use of appropriate materials science platforms. In the first part of this study,[1] we reported on an intriguing antibacterial effect caused by calcium orthophosphate (CP) nanoparticles, including hydroxyapatite (HAp) and amorphous CP (ACP). The nanoparticles were not only effective against both lab strains and clinical isolates when delivered alone, but were also able to synergize with a number of different antibiotics and significantly increase their activity against a variety of pathogenic and opportunistic bacteria, including some of the strains that are insensitive to antibiotics *per se*. The nanoparticles also exhibited a selective response whose origin was unclear: namely, while HAp was more effective than ACP against Gram-negative species and drug-resistant strains, it was not effective against Gram-positive strains, against which ACP was very effective.[1]

HAp is the most sparsely soluble nondoped CP phase and is also the mineral component of all hard tissues in the body except for the minor calcite portions of the middle ear. In contrast, ACP has been detected as the solid intermediate in the crystallization of both biogenic and synthetic HAp, forming as the result of the Ostwald law of stages, which predicts the successive formation of phases in the order of their stability. Because of its metastability, it transforms after prolonged contact with a supernatant to either HAp or dicalcium phosphate (DCP), depending on whether the terminal pH is higher or lower than ~6.8, respectively. Mammalian blood is supersaturated with respect to Hap, and the ACP units in it constantly form and dissipate, with the role in preventing their crystallization into HAp being played by α2-HS glycoprotein/fetuin-A and other serum proteins that shield individual ACP nanoparticles and prevent their aggregational growth,[2] posing along the way an intricate question of whether these omnipresent ACP units in circulation play an immune role undiscovered before. One such immune role was ascribed to Mg-enriched ACP nanoparticles forming in the ileum due to endogenous secretion of calcium and phosphate ions from the distal small intestine to the lumen, where they trap orally entered antigens and bacterial peptidoglycans

and chaperone them to the immune cells of the intestinal tissue for immunosurveillance.[3,4] Being less stable and more chemically active than HAp, ACP has been used in some dental formulations to remineralize enamel,[5] while binding with high affinity to *S. mutans*[6] and exhibiting mild anticariogenic properties whose origins are yet to be elucidated. Most of these formulations apply ACP in combination with casein phosphopeptides, providing for a rudimentary mimicry of sophisticatedly structured casein micelles stabilized in milk by ~2 nm sized ACP nanoparticles lying along the internal micelle membrane.[7] However, despite their prospect as caries-preventing additives in toothpastes and food,[8] the only metastudy of clinical trials of these formulations performed to date concluded that there was an insufficient evidence to justify the recommendation for their use in prevention of caries *in vivo*.[9] This impasse faced by CP nanoparticles as potential antimicrobials is largely due to the virtual nonexistence of studies focused on understanding their mechanism of action (MoA).

In this follow-up to the first part of the study, we shift our focus from the effect to its causes, believing that understanding the MoA of CP nanoparticles is a prerequisite for the rational optimization of their properties for an antibacterial response comparable in magnitude to today's gold standards in the domain of inorganic antimicrobials, namely, silver and, to some extent, gold, zinc, copper, and their compounds. In this attempt to decipher the MoA, we compare three stoichiometrically distinct CP nanopowders, including HAp, ACP and, to some extent, DCP. We compare them not so much to assess their individual antimicrobial potencies as to derive compositional parameters decisive in defining the MoA.

In our planning for this study, we evoked a number of testable hypotheses explaining the MoA of CP nanoparticles. One hypothesis invoked to explain the antibacterial properties of these complexes refers to their ability to adhere to dental biofilm, interfere with the binding capacity of the bacteria,[10] and also induce high intracellular free calcium ion concentrations.[11] Another possibility is that hydroxylated CP nanoparticles, such as HAp and some ACPs, act in a merely bacteriostatic fashion, thanks to their "smart" solubility in direct proportion with the acidity of the medium[12] and acid-neutralization capacity,[13] thus restricting the conditions for the growth of bacteria, including *S. mutans* and *S. aureus*, which favor mildly acidic conditions over the physiological ones.[14,15] Multiple other possibilities could be proposed, including the disruptive cell membrane effect of CP nanoparticles or Posner's clusters,[16] 9 Å sized, heavily hydrated, and nonequilibrium CP units forming the building blocks of CP nuclei and presumably constantly separating from and reintegrating with the CP surface in an aqueous medium. The formation of reactive oxygen species owing to the defective and semiconducting CP structure, as in analogy with the effect attributed to metal oxide nanoparticles constitutes another potential MoA. Therefore, in what follows, we hypothesize on a number of possible particle properties responsible for the observed antibacterial effect of CP nanoparticles and investigate them one by one. The goal of this methodology is to discern the properties of the materials responsible for eliciting the antibacterial effect, to which end it is analogous to digging a tunnel through a black box by starting from its materials science side. The results in this report will be eventually tied to its follow-up, the third and the final report of this study, which will attempt to distinguish the molecular targets in the bacterial cell vulnerable to the action of CP nanoparticles. This third and final report will be analogous to digging a tunnel through the aforementioned black box by starting from its cell biology side. The hope underlying this quest for revealing the true MoA of CP nanoparticles is that these two burrows will meet in the middle, yielding a single and consistent model connecting material properties with their biological effects.

To sum up, here we report on our effort to understand which properties of CP nanoparticles play a key role in causing this antibacterial effect by bringing three fundamentally different CP nanopowders and cements into interaction with different bacterial strains and following the bacterial response at different levels, using a range of chemical and biological assays. Better understanding of the fundamental principles underlying the antimicrobial activity of CP nanoparticles, including their MoA, is expected to be helpful in the further optimization of these nanoparticle properties and in the design of inorganic nanoparticle alternatives to small-molecule antibiotics in the global effort to curb the rising resistance of bacterial pathogens to existing therapies.

II. MATERIALS AND METHODS

A. Synthesis

Raw CP powders of different monophasic compositions were prepared as described in detail in the first part of this study.[1] Briefly, HAp [$Ca_5(PO_4)_3OH$] was synthesized by adding an aqueous solution containing 0.06 M $NH_4H_2PO_4$ and 1.75 vol. % NH_4OH dropwise to the same volume of an aqueous solution containing 0.1 M $Ca(NO_3)_2$ and 3.5 vol. % NH_4OH heated to 60–80 °C, bringing the suspension to boil, aging for 24 h, washing with water and separating the precipitate by centrifugation at 3500 rpm, and drying in air. DCP ($CaHPO_4$) was synthesized by following the same procedure except for using 0.33 M $Ca(NO_3)_2$ as the calcium solution and 0.25 M $NH_4H_2PO_4$ containing 0.05 vol. % NH_4OH as the phosphate solution and not bringing the suspension to boil. ACP was synthesized by abruptly adding a solution containing 0.5 M $Ca(NO_3)_2$ and 2 vol. % NH_4OH into the same volume of a solution containing 0.2 M $NH_4H_2PO_4$ and 1 vol. % NH_4OH, washing the precipitate first with 0.14 vol. % NH_4OH, then with ethanol, drying in air, and storing at 4 °C to prevent spontaneous transformation to HAp. ACP and HAp cements were prepared by mixing 10 mg of the corresponding dry powders with 15 μl Na_2HPO_4, homogenizing the mixture manually and immediately depositing it either onto agar plates or into bacterial broths.

B. Physicochemical characterization

Zeta potential and hydrodynamic diameters of particles in suspension were measured in a dip cell using a Zetasizer Nano-ZS (Malvern) dynamic light scattering device. To create ξ-potential versus pH curves, titration with 1 M HCl proceeded from the physiological pH to higher pH values with one sample and from the physiological pH to lower pH values with another identical sample. The morphology of the CP nanopowders was analyzed on a Hitachi S-4300SE/N scanning electron microscope (SEM) at the Lawrence Berkeley National Lab, with the electron beam energy of 15 kV. Particle size distribution histograms for the different types of cements and HAP precursors were obtained from scanning electron micrographs using IMAGEJ (NIH, Bethesda, MD) and the sample size of 200–1000 particles. X-ray diffraction (XRD) studies were carried out on a Siemens D500 diffractometer using $Cu_{K\alpha} = 1.5418$ Å as the wavelength of the radiation source, the step size of 0.04°, and 1 s of sample irradiation time per step. The UV–Vis diffuse reflectance spectra were collected in the 200–800 nm wavelength range on an Agilent Cary 5000 spectrophotometer equipped with a diffuse reflectance accessory. Photoluminescence (PL) spectra were recorded on a Horiba Jobin Yvon Fluorolog FL3–22 spectrofluorometer using Xe lamp excitation with the wavelength of 325 nm. Luminescence photographs of ACP and HAp under the 405 nm wavelength irradiation in dark were taken by a digital camera.

C. Calcium assays

Calcium release analyses were done by immersing 10 mg of powders in 10 ml of 20 mM Bis-Tris aqueous solution (pH 6.8) and measuring the solution potential using the Ca^{2+} microelectrode in combination with a reference electrode (Microelectrodes, Inc.) on an Accumet pH-meter (Fisher Scientific). Calibration solutions were prepared in the same solvent using $CaCl_2$ in the 1 μM–100 mM concentration range. Calibration data points were exponentially fitted in the 1 μM–1 mM $CaCl_2$ (OriginPro 2016), and the numerical fit was used to convert the electrode potential readings into free Ca^{2+} molar concentrations. All the samples were analyzed in triplicates and compared against the control samples. Free intracellular Ca^{2+} concentrations were measured using Fura-2 assay and a modified version of an older protocol. For that purpose, the overnight cultures of *E. coli* treated with 60 mg/ml of either ACP or HAp nanoparticles first had the particles dissolved by centrifuging 200 μl of the suspension and resuspending in 200 μl of 110 mM solution of NaCl in 250 mM HCl. After the particles were removed, the pH was brought back to neutral by centrifuging and suspending in buffer A. The bacteria were then permeabilized to Fura-2 dye by resuspending in 0.12 M Tris-HCl (pH 8) solution containing 200 μM EDTA at 37 °C for 2 min and adding $MgCl_2$ to the final concentration of 1 mM to stop the reaction, after which the bacteria were centrifuged and washed once with buffer A. After permeabilization, bacteria were incubated in 5 μM Fura-2 pentaacetoxymethyl ester in buffer A at 37 °C for 2 h, after which the volume of the suspension was increased by adding 25 times more buffer A, centrifuging and washing 3× with buffer A. Suspensions were excited at 340 nm, and the emission was measured at 510 nm. Increased intracellular free calcium ion concentration, $[Ca^{2+}]_i$, corresponds to a higher emission under the 340 nm excitation compared to the control and the following equation was used to convert the fluorescence at 510 nm, *F*, in the CP-treated samples to $[Ca^{2+}]_i$:

$$[Ca^{2+}]_i = K_d \times (F - F_{min})/(F_{max} - F). \quad (1)$$

The value of 225 nM was taken for the dissociation constant for Fura-2, K_d.[17] The bacterial cell control permeabilized with 25 μM gramicidin was used to measure F_{max}, and the bacterial cell control incubated with Ca^{2+}-chelating agent, 10 mM ethylene glycol tetraacetic acid, was used to measure F_{min}.

D. Antibacterial assays

Antibacterial assays performed by dispersing nanoparticles in Luria broths (LB) and by depositing them on LB agar plates were described in the first part of the study.[1] Briefly, 1 ml of 1:50 diluted overnight cultures of bacteria mixed with CP nanopowders were incubated overnight at 37 °C and 200 rpm, with or without the presence of concomitantly added antibiotics. After the overnight incubation, 200 μl of the bacterial suspension was centrifuged at 10 000 rpm and resuspended in 200 μl of 110 mM solution of NaCl in 250 mM HCl (150 μl 0.85 wt. % mixed with 50 μl of 1 M HCl) to dissolve the CP nanoparticles and avoid their interference with the optical density readings. All experimental sample groups and controls were subjected to centrifugation and HCl treatments. In the agar diffusion antibacterial assays, 5 mg of CP nanopowders were placed onto a bacterium-infused LB agar plate with the spot radius of 1 cm. The agar plates were incubated for 24 h at 37 °C, after which the radius of the zone of inhibition was used to gauge the antibacterial activity of the cements. All the samples for both antibacterial assays were analyzed in triplicates. Experiments involving concomitant UV irradiation of broths with and without the ACP powder were performed by placing 1 ml of control broths or broths containing 90 mg/ml ACP into Shimadzu Q71483 UV/Vis spectrophotometer and irradiating for 5 min with the laser light wavelength of 220 nm, after which they were aged overnight on the shaker at 37 °C and had optical densities at 600 nm, indicative of the bacterial viability, measured (BMG LABTECH FLUOstar Omega) and converted to the number of colony forming units (CFU) by multiplying with 8×10^8.

E. Drug loading and release

The concentrations of vancomycin, erythromycin, and ampicillin loaded onto CP particles and released after 24 h was determined by creating a standard curve of agar plate inhibition zones versus antibiotic concentration in the 0.075–20 mg/ml range and then comparing it with the zone created by a given amount of antibiotic-loaded CP particles.

Binding of *E. coli* derived lipopolysaccharide (LPS, VWR) onto CP nanoparticles was determined by incubating 5 mg/ml HAp or ACP nanoparticles in 40 mg/ml LPS solutions in water and measuring the optical density at 280 nm after 1 h and also taking the FTIR spectra of the corresponding precipitate obtained following centrifugation. LPS loading efficiency, x, was defined as

$$x = m_{(LPS)}/m_{(CP)} \times 100\%, \quad (2)$$

where $m_{(LPS)}$ is the mass of LPS bound onto CP and $m_{(CP)}$ is the mass of CP. LPS binding, y, efficiency was defined as

$$y = m_{(LPS)}/m_{T(LPS)} \times 100\%, \quad (3)$$

where $m_{(LPS)}$ is the mass of LPS bound onto CP and $m_{T(LPS)}$ is the total mass of LPS.

III. RESULTS AND DISCUSSION

In the effort to delineate the key structural effects responsible for the antibacterial properties of CPs, nanoparticles of three chemically and crystallographically different CP phases were compared: (i) hydroxylated HAp, the CP phase comprising the mineral component of mammalian bone tissues; (ii) hydrogenated DCP, a CP phase forming in acidic solutions and strictly found in pathogenic calcified tissues; and (iii) ACP, a phase that is highly active, metastable, and quick to transition to HAp, acting as is its precursor in the process of biomineralization. Figure 1 displays SEM micrographs and x-ray diffractograms of HAp and ACP, the two main nanomaterials used in this study, demonstrating high levels of morphological similarity, but different crystallinities. Their more detailed physicochemical characterization, such as particle size, morphology, crystallinity, phase composition, and thermal stability, including the basic information about their antibacterial efficacy and selectivity, was given in the first part of this study.[1]

This section follows an innovative, but logical form by being divided to nine subsections, each dealing with the investigation of a single effect potentially causative of the observed antibacterial activity and ending up with an estimate of how realistic and/or critical its role in the process is. This approach is justified by the fact that will become obvious in the course of the discussion: rather than a single particle property being the determinant of the antibacterial effect, a number of them acting in synergy are responsible for causing this effect. The findings resulting from the approach based on analyzing the effects of one variable at a time are limited by the fact that these different variables cannot be fully disentangled from one another. For example, with changes in crystallinity, the surface composition, the structural water content, faceting, and diffusivity all change as well, even when the particle size and shape, as is the case here, are maintained constant. Likewise, in the attempt to modify the surface defect concentration using a high-temperature treatment, both crystallinity and the surface ion/cluster exchange dynamics across the particle/solution interface are modified too. Also, with an increase in the particle size, the surface curvature and, thus, the interfacial free energy change as well, affecting an array of properties directly or indirectly dependent on it. Notwithstanding this fundamental limitation, one such discernment of possible factors and their analysis are carried out with the expectation that they will present the basis for the future optimization and design of CP nanoparticles for the exhibition of a maximal antibacterial activity against medically relevant pathogens.

A. Calcium ion release

The antibacterial activity of silver nanoparticles is usually attributed to their intracellular dissolution and release of Ag^+ ions that inhibit DNA replication and inactivate ribosomal subunit proteins and enzymes involved in respiration and adenosine triphosphate (ATP) production.[18–20] It is tempting to imagine that CPs share a similar MoA. Accordingly, Ca^{2+} ions released by the CP particles would have the ability of eliciting a toxic effect on the bacterial cells, similarly to the mechanism that they have been hypothesized to owe their

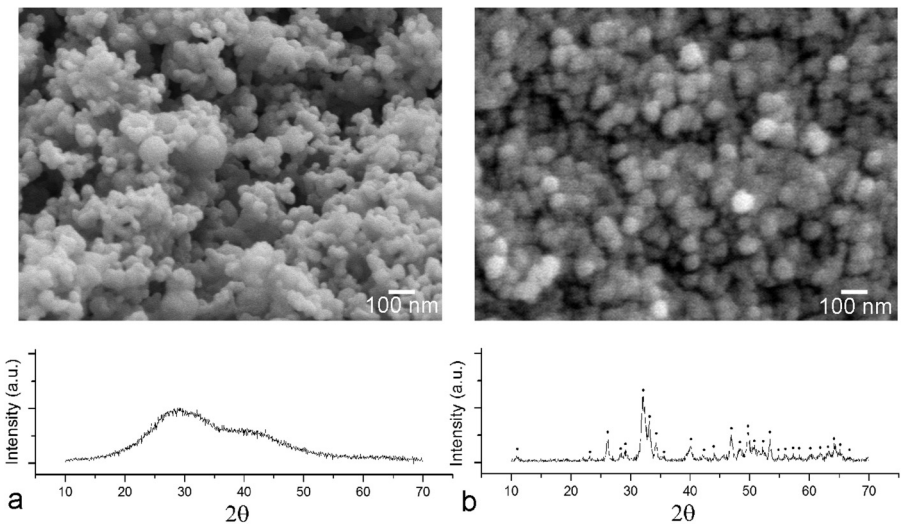

FIG. 1. SEM images and XRD patterns of ACP (a) and HAp (b) nanoparticles. Diffraction peaks labeled with • originate from HAp.

capacity to deteriorate the eukaryotic cells to.[21,22] Hence, our initial hypothesis was that the discrepancy between the high activity of ACP and the low activity of HAp against *S. aureus* reported in the first part of this study[1] may be explained by the higher solubility of ACP (0.8 g/ml) in physiological media than that of HAp (0.3 g/ml)[23] and the consequently more copious release of Ca^{2+} ions by ACP than by HAp. In support of this hypothesis, we recalled that carboxylic moieties of peptidoglycans and polyphosphate groups of teichoic acid (TA) comprising the cell wall of Gram-positive bacteria provide the binding sites for Ca^{2+} and other metal ions.[24] Earlier research showed that Ca^{2+} ions delivered as $CaCl_2$ salt had a deadly effect on *S. aureus* at ≤40 mM by promoting Ca^{2+}-cardiolipin binding and decreasing the membrane curvature, thus destabilizing and eventually destroying it.[25] Per this research, this effect was absent in *E. coli* and *B. subtilis*, presumably because of the thinner proteoglycan cell membrane layer and the double cell wall in the latter. If realistic, this susceptibility of TA toward inactivation by Ca^{2+} ions would also explain the efficacy with which $Ca(OH)_2$ particles, relying mostly on Ca^{2+} ions to elicit the antibacterial effect, are used as endodontic medicaments in dentistry.[26] It might also explain why bacteremic patients are diagnosable with hypocalcemia in particular clinical circumstances,[27] a possible result of the recruitment of Ca^{2+} ions from the serum to the site of infection to assist in neutralization of the pathogenic cells.

To test whether ionic calcium is the "culprit," the antibacterial effect of sole Ca^{2+} ions in concentrations equivalent to those released by CP nanoparticles in PBS was measured on *S. aureus* and *P. aeruginosa*. Based on the current solubility analyses [Figs. 2(a) and 2(b)], agreeing with the previous ones,[28] the 10–100 mg/ml range for ACP corresponded to 4–40 mM of Ca^{2+} concentration range using a water-soluble calcium salt, $CaCl_2$. However, no parallel decreases in viability

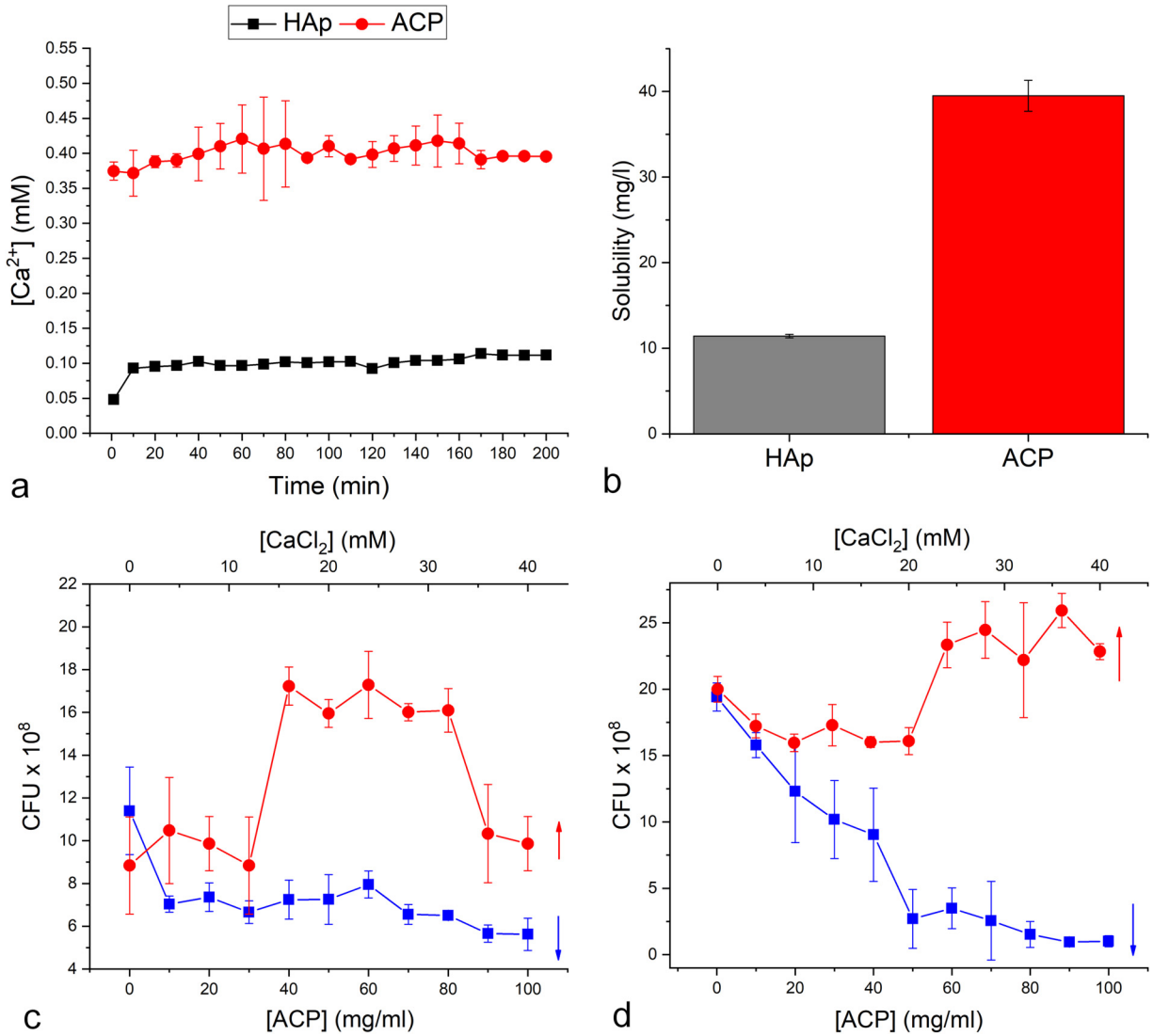

FIG. 2. Time-dependent release of free calcium ions due to dissolution of different CP phases at 1 mg/ml (a) and solubility in a solution equilibrated after aging the precipitate for 3 h (b). Data points represent averages (n = 3) and error bars represent the standard deviation. Comparison of *P. aeruginosa* (c) and *S. aureus* (d) viabilities in the 4–40 mM range of $CaCl_2$ and in the 10–100 mg/ml range of ACP. Data points represent averages (n = 4) and error bars represent the standard deviation. Arrows in (c) and (d) denote abscissas that the individual curves correspond to.

of populations treated with comparable concentrations of ACP and $CaCl_2$ were noticed for either of the two bacterial species tested [Figs. 2(c) and 2(d)]. As a matter of fact, the viability of both types of bacteria increased as the free Ca^{2+} concentration went up. Moreover, the viability of broths treated with the nanoparticles was consistently lower than that of the broths challenged with the comparable levels of free Ca^{2+} ions. This has proven that Ca^{2+} ions *per se* cannot be the sole bearer of the antibacterial activity of CPs. Though their effect cannot be discarded with certainty, at best it is delivered in synergy with one or more CP particle properties. Higher concentrations of calcium released in the ionic form upon the treatment with ACP might destabilize the cell wall and make the cell susceptible to a complementary antibacterial effect delivered by the particles. Their ability to open up the mechanosensitive ion channels and facilitate the intracellular delivery of the nanoparticles is also a possibility.

Another possibility is that the uptake and intracellular degradation of particles increases free calcium levels beyond those resulting from the rather sparse dissolution in regular media. *E. coli* is capable of maintaining $[Ca^{2+}]_i$ homeostasis at ~100 nM even when the extracellular levels exceed 10 mM,[29] but if internalized and degraded intracellularly, CP particles could theoretically flood the cell with Ca^{2+} and induce damage to it. To test if the uptake of the particles and their intracellular dissolution is the mechanism for increasing $[Ca^{2+}]_i$ to toxic levels, Fura-2 analysis was performed on *E. coli* challenged with 60 mg/ml ACP or HAp. At this dose, which exceeded the IC_{50} value for HAp and equaled that of ACP, $[Ca^{2+}]_i$ increased twofold, from 111.5 ± 9.4 nM in the control *E. coli* to 215.7 ± 9.9 nM inside ACP-challenged *E. coli* and 248.3 ± 18.3 nM inside HAp-challenged *E. coli* (Fig. 3). ACP is more soluble than HAp and two effects are at work that explain the somewhat higher $[Ca^{2+}]_i$ in HAp-treated *E. coli*: (1) ACP comprises 22.2 wt. % of lattice water as opposed to only 6.6 wt. % for HAp (Ref. 1) and (2) the 60 mg/ml CP dose is equal to the IC_{50} of ACP, but twice higher than the IC_{50} of HAp. Also, countering the expectations, there is evidence that ACP can be stabilized intracellularly, presumably due to the high concentration of Mg^{2+} ions and ATP,[30] rather than swiftly transforming to HAp or dissolving in the digestive compartments of the cell. All these arguments imply a higher potential for cytosolic leakage and CP/Ca^{2+} entrance into the cell in HAp-treated bacteria than in ACP-treated ones. Still, although higher than the control, the intracellular Ca^{2+} levels were within the range of resting cytosolic $[Ca^{2+}]_i$ of *E. coli*, which can tolerate $[Ca^{2+}]_i$ peaks reaching 1–5 μM.[31] Therefore, the increased level of intracellular ionic calcium may destabilize the bacteria and make them susceptible for the action of other factors, but it, itself, cannot be responsible for the elicitation of the antibacterial effect.

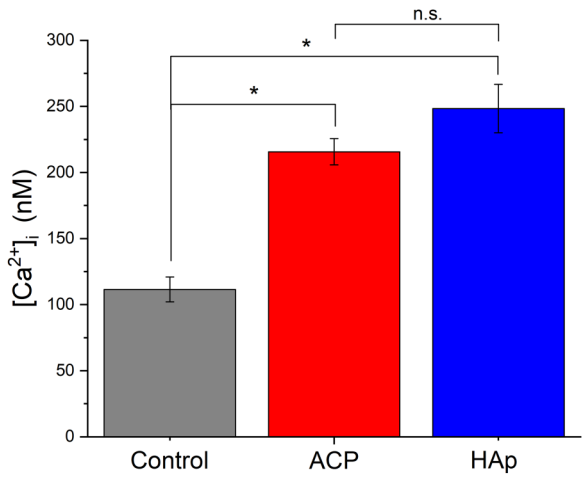

FIG. 3. Intracellular free Ca^{2+} concentration in control *E. coli* populations and populations challenged with 60 mg/ml ACP or HAp measured using the Fura-2 assay. Data points represent averages (n = 3) and error bars represent the standard deviation. Data points statistically significantly lower ($p < 0.05$) compared to other data points are marked with an asterisk. Data points statistically insignificantly different ($p > 0.05$) compared to other data points are marked with "n.s."

This conclusion is backed by the significant difference observed in the effect of ACP and HAp depending on whether the bacteria were Gram-positive or Gram-negative, suggesting that ACP and HAp must have a different MoA. Such different modes of action were previously ascribed to nanoparticles with identical compositions, but produced using different methods, one of which were carbon nanoparticles.[32] This difference in the MoA implies that a particle-related effect must be the key to mechanistically explaining the activity of CPs, given that the dissolved units of ACP and HAp would be qualitatively indistinguishable. Since the toxic influence of phosphates and hydroxyls, the other two ionic species in HAp, is also less probable than those of Ca^{2+}, these have been the first out of many indications that not ions, but particles exhibit properties responsible for the antibacterial activity. Indirectly, also, the observed discrepancy between the activities of ACP and HAp is the first indicator of a multifactorial nature of the antibacterial activity of CP nanoparticles.

B. Surface charge

In contrast to the global surface charge distribution, electrodynamic characteristics of the double charge layer of ACP and HAp are expected to be very different. A comparative analysis of ξ-potential as a function of pH for ACP and HAp showed that the ξ-potentials at the physiological pH were negative for both materials, but their absolute values were higher for HAp than for ACP: −12.5 versus −9 mV, respectively. Interestingly, HAp is more receptive to negatively charged ions in its double layer, allowing for the ξ-potential to drop to more negative values in the alkaline pH range than ACP, while ACP is more receptive to positively charged ions in its double layer, allowing for the ξ-potential to enter the positive value range under the acidic conditions [Fig. 4(a)]. Specifically, in the entire pH range between the point of zero charge (PZC) at 5.75 and the onset of dissolution at pH 3–4, the ξ-potential of HAp is positive, but does not increase above 0.2 mV, whereas that of ACP exceeds 4 at pH 4.9.

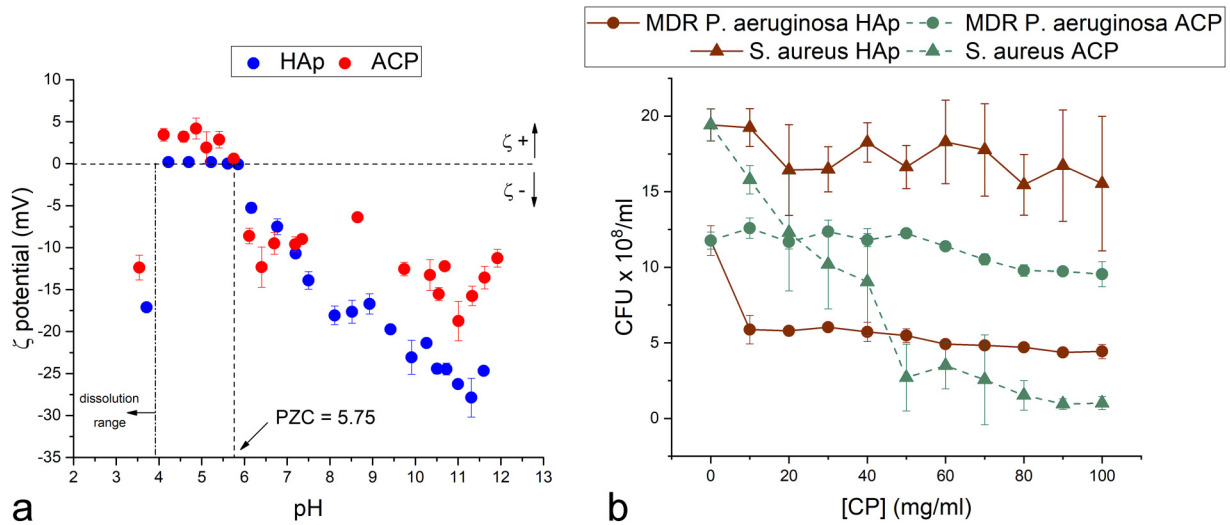

FIG. 4. (a) Zeta potential vs pH titration curves for HAp and ACP colloids in the 3.5–12 pH range. Phosphate buffered saline (1x), containing 137 mM NaCl, 2.7 mM KCl, 10 mM Na_2HPO_4, and 1.8 mM KH_2PO_4, was used as the medium. Dissolution range is entered at pH < 4, while PZC stands for the point of zero charge. Data points represent averages (n = 3) and error bars represent the standard error of the mean ($SD/n^{1/2}$). (b) Comparative curves showing the reduction in the concentration of bacterial CFU with the concentration of HAp or ACP in broths for one Gram-negative clinical strain, namely, MDR *P. aeruginosa*, and one Gram-positive lab strain, namely, *S. aureus*.

The gradual dissolution of both materials begins at pH < 4.0, at which point the ξ-potential abruptly drops to values lower than −10 mV, intensely negative despite the excess of protons in the medium. This effect is expected to be the result of the selective dissolution favoring the release of lighter, cationic Ca^{2+} before the degradation and dissipation of the network of heavier phosphate ions. The same atomic weight argument can be used to explain a similar excess of phosphate ions in the solid phase during the earliest stages of nucleation and crystal growth[33] as well as the fact that the formation of HAp from amorphous precursors is correlated to the activity coefficient and speciation of the phosphate ion.[34]

In theory, the moderate negative charge of both ACP and HAp nanoparticle surfaces under the physiological conditions may allow for the electrostatic attraction of the nanoparticles to the peptidoglycan layer rich in cationic alanine and lysine residues surrounding the cell wall of Gram-positive bacteria and to the core polysaccharides sticking out of the outer membrane of Gram-negative bacteria, rich in different cationic species, i.e., 4-aminoarabonises and phosphoethanolamines.[35] If this was correct, however, then the different modes of action of ACP and HAp, such as those presented in Fig. 4(b), could not be explained on the basis of surface charge effects and the relevancy of this parameter would have to be excluded *ab absurdum*.

A more plausible scenario where surface charge would have some antibacterial effect involves electrostatic repulsion, not attraction. Namely, with the electrostatic repulsion barrier being the first one that must be crossed by a nanoparticle *en route* to the bacterial cell surface, the somewhat lower surface charge of ACP might favor the interaction with the cell wall over HAp. Presumably caused by a higher content of adsorbed and lattice water in ACP than in HAp, this lower surface charge may also facilitate the transport of the nanoparticle across the cell membrane, as in gene delivery, alongside acting as its potential disruptor, thus explaining the discrepancy between the antibacterial activity of these two forms of CP. One thing that is not clear is whether the relatively small difference in the ξ-potential at this pH, amounting to only 3–4 mV, is sufficient to justify the expectation of a more intense hydrophobic barrier permeation propensity of ACP.

When it comes to the propensity to traverse or adhere to the biological barriers, including the cell wall and plasma membrane, negative surface charge is a hindrance, especially against phospholipid bilayers inherently incompatible with the hydrophilic nature of CPs, comprising two relatively highly charged ionic species: divalent calcium and trivalent phosphate. Although cationic surfaces tend to have more pronounced antibacterial properties,[36] combining cationic and anionic species on the surface, such as those present on the surface of CP, can retain the antibacterial efficacy while regaining better tissue compatibility,[37] and this duality is exactly the strength of CPs. Zwitterionic surfaces, in fact, are known for their excellent antifouling properties, which they owe to the tight hydration shells formed around charged groups.[38] Water within this shell has a greater resemblance to free water than hydrogen-bonded water around simply hydrophilic groups, such as those of poly(ethylene) glycol (PEG), and its structuring during the penetration of a foulant is even less entropically favorable than that around PEG, the epitome of an excipient for reduced opsonization. CPs may similarly owe a portion of their antibacterial activity to the alternation of relatively highly charged ionic species on an equally highly hydrated surface. Their activity may be due to the synergy of a translationally symmetric order of two species, Ca^{2+} and H_xPO4^{x-3}, that separately have a significantly lesser antibacterial potency. It is widely known that the

antifouling properties of zwitterionic materials most critically depend on the surface charge distribution,[39] and it is conceivable that a different distance between constitutive ions on the surfaces of ACP and HAp—with the caveat that ACP transforms to HAp after sufficient aging in physiological solutions and that its surface may structurally bear resemblance to HAp all the way through—may endow these two materials with vastly different antibacterial properties and be a key to explaining their different specificities against particular families of microorganisms. The translational symmetry of surface features often has a more pronounced effect on the biological response than the features *per se*[40] and whether these distances between charged species on the surface of CP nanoparticles could be optimized to provide for a more superior antibacterial effect is a meaningful question to ask at this point.

To sum up, there are valid arguments in favor of the low surface charge and its zwitterionic distribution as potential antibacterial factors. The combination of low net charge and high charge density is intriguing and may be harnessed to induce intense interactions with cells. However, a minimal difference in the ξ-potential versus pH profiles and the identical PZC for both materials, 5.75, suggests similar electrostatic properties of their surfaces and excludes simple electrostatics as the key antibacterial factor, lest the difference in the activity of these two materials remains unexplained. This lateral role of sheer electrostatics is further supported by the fact that despite the lower absolute value of the ξ-potential, ACP particles are markedly more colloidally stable than HAp. This observation hints at the critical role of surface effects other than the long-range electrostatic, e.g., the diffusion of ionic units and clusters in the double charge layer. Although surface charge may lower the energy barrier for nanoparticles coming into contact with the cells, expecting that this physical factor alone is sufficient to induce the antibacterial effect would be overly simplistic and unrealistic. The electrostatic force is a nondirectional, long-range force and is but a crude prelude to finer, albeit weaker forces that govern interactions at the molecular and nanoscales with higher levels of specificity.[41]

C. pH changes

The constantly ongoing process of dissolution and reprecipitation on the HAp surface entails constant pH fluctuations in the nanoscopic medium surrounding the particle and it can be hypothesized that such fluctuations could destabilize microorganisms. Equations (4) and (5) simplistically describe the pH effects accompanying the dissolution and reprecipitation of one unit cell of HAp, respectively,

$$Ca_{10}(PO_4)_6(OH)_2 + 6H_2O \rightarrow 10Ca^{2+} + 6HPO_4^{2-} + 8OH^-, \quad (4)$$

$$10Ca^{2+} + 6HPO_4^{2-} + 2H_2O \rightarrow Ca_{10}(PO_4)_6(OH)_2 + 8H^+. \quad (5)$$

Figure 5 shows changes in the pH of deionized water following immersion of the three different CPs. The most stable phase was, expectedly, HAp, not exhibiting any significant dissolution, which would have been entailed by a pH increase from the neutral level. The solubility of DCP was dependent on the thermal treatment during the synthesis. Without the thermal treatment that involved the bringing of the suspension to boil after precipitation to block the particle surface, DCP proved to be the most soluble CP phase, exhibiting the most intense pH drop, down to 5.17 ± 0.01 after 7 h of aging. With the thermal treatment, the solubility of DCP was lesser and this difference between the two forms of DCP indirectly proves that the pH drop is due to the transformation of amorphous surface layers to HAp/DCP in water rather than due to dissolution of DCP. In fact, although DCP

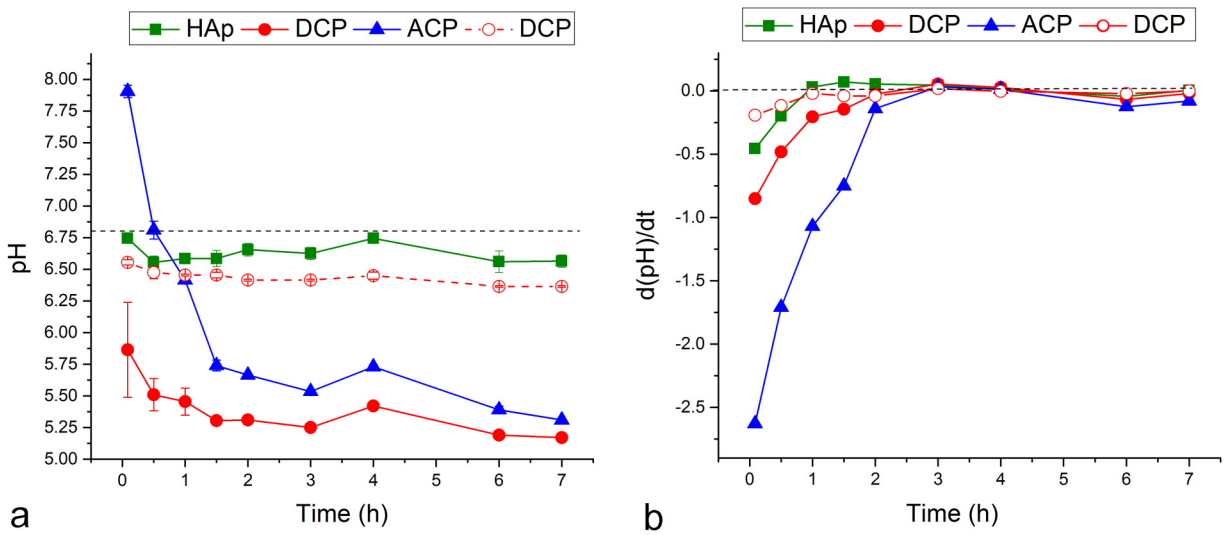

FIG. 5. Absolute (a) and differential, dy/dt (b) change in the pH of the supernatant in a 20 mg/ml dispersion of different CP nanopowders in water at 37 °C over time. Dashed lines in (a) and (b) denote the neutral pH at 37 °C and the zero change in pH over time, respectively. Full and empty red circles denote data points for DCP not subjected and subjected to the thermal treatment (bringing of the precipitate to boil), respectively. Data points represent averages (n = 3) and error bars represent the standard deviation.

is colloquially known as an acidic form of CP, dissolution of DCP would exert the same effect on pH as the dissolution of HAp, albeit less intense, the reason being the alkaline nature of the released amphoteric HPO_4^{2-} ion (pKa = 7.2) under neutral conditions (pH 6.8 at 37 °C). pH has to exceed 10 in order for HPO_4^{2-} ion to be acidic, unlike pH 4.7 for $H_2PO_4^-$, explaining why monocalcium phosphate, $Ca(H_2PO_4)_2$, is the only true acidic form of CP. This is why precipitation of DCP was paralleled by a decrease in the pH, as was the case of HAp. Because of its metastable structure, the most unstable CP phase was ACP. It exhibited a drop in the pH, down to 5.31 after 7 h, which was similar, but somewhat less intense as that seen for DCP, the reason being the release of free protons following the capture of OH^- groups into HAp forming as the result of dissolution/reprecipitation process taking place on the surface of ACP [Eq. (5)]. The increase of pH in the ACP supernatant from the starting neutral value to 7.90 ± 0.05 (the first time point) almost immediately as the solid phase was brought into contact with the solution can be explained either by the apatitic surface of ACP dissolving first and raising pH, before exposing the $Ca_3(PO_4)_2$ interior and its subsequent, more gradual transformation to HAp, or by the initial formation of octacalcium phosphate (OCP) as an intermediate in the formation of HAp. Namely, ACP → OCP transformation would lead to the release of six hydroxyl groups from the solution per the unit cell of OCP [Eq. (6)]. Per Eq. (7), the subsequent transformation of OCP to HAp would produce a steeper drop in pH than that excepted from direct ACP → HAp transition [Eq. (8)], i.e., 1.5 protons vs 0.667 protons per the stoichiometric unit of HAp, respectively. The differential curves demonstrate the largest degree of pH change occurring in the solution interfaced with ACP, confirming that its propensity toward phase transitions and exchange of material with the medium is significantly more pronounced than that of HAp or DCP,

$$8Ca_3(PO_4)_2 \times 3H_2O + Ca_3(PO4)_2 + 8H_2O \rightarrow 3Ca_8H_2(PO_4)_6 \times 5H_2O + 3Ca^{2+} + 6OH^-, \quad (6)$$

$$5Ca_8H_2(PO_4)_6 \times 5H_2O + 3H_2O \rightarrow 8Ca_5(PO_4)_3OH + 6HPO_4{}^{2-} + 12H^+, \quad (7)$$

$$4Ca_3(PO_4)_2 \times 3H_2O + Ca_3(PO_4)_2 \rightarrow 3Ca_5(PO_4)_3OH + HPO_4{}^{2-} + 2H^+. \quad (8)$$

To test if the release of protons is responsible for the elicitation of the antibacterial effect, the activity of ACP and DCP, the two proton-releasing CP phases analyzed here, was tested in parallel. The activity of DCP not subjected to the thermal treatment was higher than that of ACP against *E. coli* in the high concentration range, but significantly lower against *S. aureus* and *P. aeruginosa* in the entire range of concentrations (Fig. 6). The fact that DCP acidifies the medium most, but has a more viable effect on *S. aureus* and *P. aeruginosa* than ACP refutes the idea that the release of protons following the reprecipitation of CP growth units that transiently separate, like a comet tail, from the particle surface is solely responsible for the antibacterial effect. The lack of effect of the local pH drop caused by the surface dissolution and reprecipitation is in agreement with the similar inability of polyesters to elicit antimicrobial effects solely due to their mild acidity.[42] The idea that the release of protons cannot be the decisive antibacterial factor *per se* is additionally supported by the fact that the activity of HAp, whose proton-releasing capacity should be significantly lower than that of ACP, was absent against *S. aureus*, but comparable and per some criteria, e.g., IC_{50}, even higher than that of ACP. Besides, carbonates and phosphates, along with amino acid side chains and terminal groups capable of undergoing protonation/deprotonation, should effectively buffer the H^+/OH^- imbalance of this, relatively minor degree and prevent their adverse effects on protein structure and stability. One such buffering capacity of tissues explains why alkalization achieved by relatively soluble $Ca(OH)_2$ is effective only against bacteria on open surfaces, but not inside tissues, even when they are relatively low in cellular count, such as dentin or the root

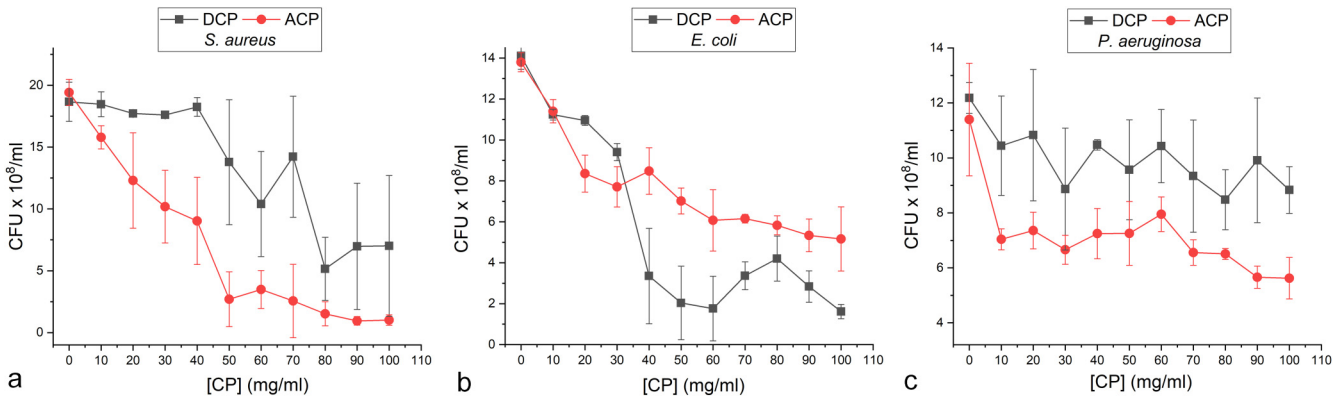

FIG. 6. Reduction in the concentration of colony forming units of *S. aureus* (a), *E. coli* (b), or *P. aeruginosa* (c) in broths treated with ACP or DCP nanoparticles in the 0–100 mg/ml concentration range. Data points represent averages (n = 3) and error bars represent the standard deviation.

canal, where the high pH produced by $Ca(OH)_2$ is usually buffered and kept in the physiological range.[43]

D. Particle size

It is widely known that particle size has a powerful effect on biological properties, even more so when nanomaterials are compared to their bulk analogues.[44] Even within nanomaterials, fine variations in the particle size can produce humongous differences in the biological response to these materials.[45] As far as antimicrobial silver is concerned, the sub-10-nm particles were reported to be more effective than the bigger units.[46] To test whether the particle size has an effect on the antibacterial activity of CPs, the activity of HAp and ACP powders against planktonic *P. aeruginosa* was compared to the activity of their dry cements, which were typified by different particle size histograms and average particle sizes. Namely, while the particle size distribution in HAp powders and dry cements was similar [Fig. 7(a)], the average particle size was somewhat larger in HAp powders than in cements [Fig. 7(c)]. In contrast, the particle size in ACP powders was significantly smaller than in dry ACP cements [Figs. 7(b) and 7(c)]. Whereas in the case of HAp, no phase transition accompanies the cement formation process and the introduction of the liquid phase and agitation manage merely to break down the fine particle agglomerates, crystallization parallels the cement formation from the ACP precursor, resulting in grain coalescence and growth. Planktonic *P. aeruginosa* was chosen for this assay because of the relatively minor difference in the efficacy of ACP and HAp powders against it.[1] Dispersed in the inoculated broths, all powders significantly reduced the bacterial population growth, even at the lowest tested concentration of 10 mg/ml [Fig. 7(d)]. More importantly, however, the antibacterial effect of ACP cement was consistently lower than that of the corresponding powder and the effect was opposite

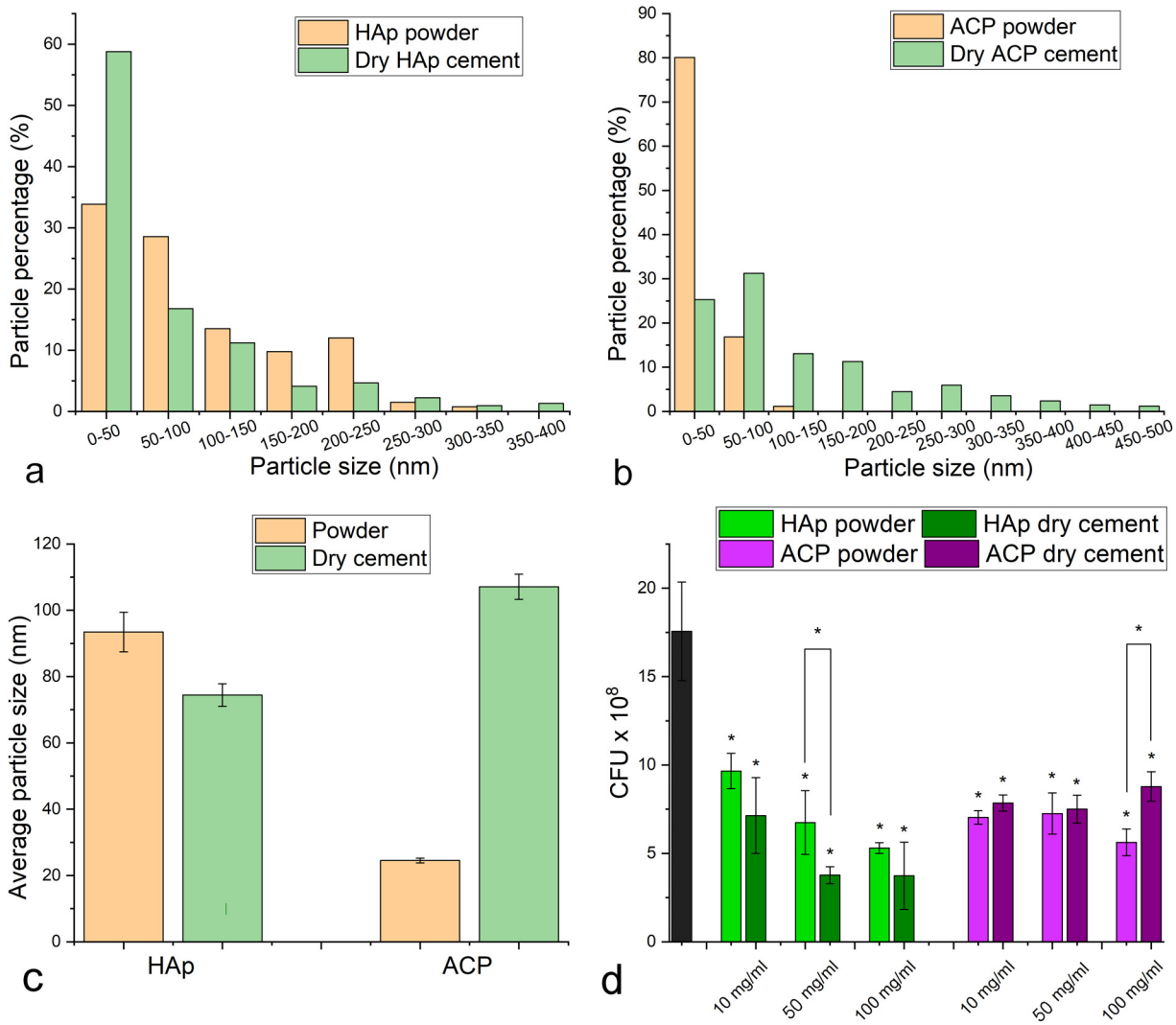

FIG. 7. Comparative particle size distribution histograms [(a) and (b)] and average particles sizes (c) for HAp [(a) and (c)] and ACP [(b) and (c)] powders and dry cements, and the comparison of the concentration of *P. aeruginosa* colony forming units per ml of the bacterial broth treated with HAp powders or dry cements at the concentrations of 10, 50, and 100 mg/ml. Data points represent averages ($n = 3$) and error bars represent standard error of the mean in (c) and standard deviation in (d). Data points statistically significantly lower ($p < 0.05$) compared to the control, untreated population are marked with an asterisk.

for HAp. For both ACP and HAp, the solids containing smaller particle sizes (ACP powder and HAp cement) exhibited a more pronounced antibacterial effect than their analogues containing larger particle sizes. With the average particle size being on the nanoscale, i.e., <100 nm, for all the systems, these findings indicate that the nanoparticulate nature of CPs is an important prerequisite for their exhibition of optimal antibacterial activities. Indirectly, the fact that there was a difference in the treatment outcome depending on the particle size reiterates the aforementioned point that particles, not merely ions, must elicit properties that induce the antibacterial effect. This reinforces our hope that materials science can be used to craft therapies that equal or surpass in effectiveness those of traditional antibiotics and other molecular pharmacotherapies.

E. Crystallinity

Because of the lower interfacial energy, amorphous particles are absorbed systemically faster than their crystalline counterparts.[47] However, there is no model proposing a general difference between crystalline and amorphous modifications of particles in terms of their biological effects at the cell level. Still, prior research has shown that the amorphous phase of CP exhibits an increased activity in cell culture compared to any crystalline modifications.[48] Also, as demonstrated by the clear difference in the antibacterial activities of HAp and ACP against particularly Gram-positive bacteria and by the selective engagement of ACP or HAp into synergies with specific antibiotics, crystallinity has a definite effect on the antibacterial properties of CPs.[1] Only one effect is presented here, concerning the selective engagement of only ACP, but not HAp, in synergy with vancomycin against *P. aeruginosa*, activating this antibiotic, which is otherwise ineffective against this bacterium, and making it very effective in inhibiting the bacterial growth. Thus, whereas the combination of vancomycin and HAp does not lower the bacterial colony count in broths at all, the combination of vancomycin and ACP reduces it by 80% already at the very small ACP dose of 0.5 mg/ml (Fig. 8). For each particle concentration tested in the 0.5–20 mg/ml range, there is a statistically significant to extremely significant difference in the effect of these two combination therapies (Fig. 8). Crystallinity, however, presents mainly a bulk phenomenon and only its effect on the surface processes, which come into direct contact with the bacteria, is expected to be important. Surface, of course, is defined as the first 10–20 atomic layers and itself presents but a different kind of a bulk phenomenon. As will be pointed out in further sections, crystallinity is not simply proportional to the antibacterial activity; rather, the fact that ACP is more effective against Gram-positive lab strains and HAp against the multidrug-resistant (MDR) analogues suggests that ACP and HAp must be typified by thoroughly different mechanisms of action.

F. Structural metastability and surface defects

In the next stage of this study, we wanted to explore whether UV light, in analogy to the effect it causes in

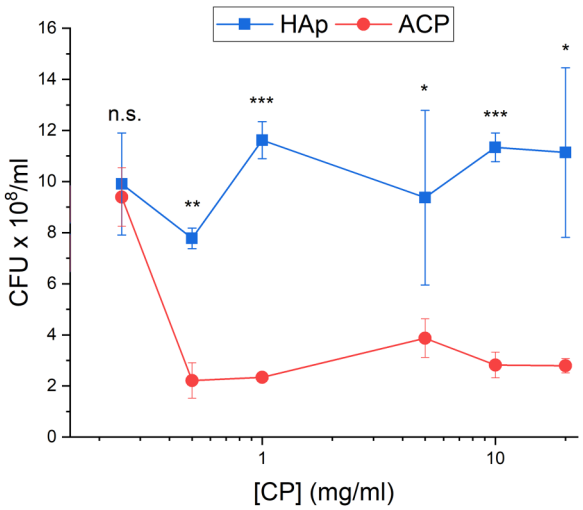

FIG. 8. Broth concentration of colony forming units of *P. aeruginosa* treated synergistically with different concentrations of ACP or HAp nanoparticles and 100 mg/ml of vancomycin. Data points represent averages (n = 3) and error bars represent the standard deviation. Different levels of statistically significantly difference between the concentration of colony forming units in HAp- and ACP-treated broths are marked with * if significant ($p < 0.05$), ** if highly significant ($p < 0.001$), or *** if extremely significant ($p < 0.0001$).

inorganic antibacterial materials with photocatalytic properties, such as titanium oxide and zinc oxide, can augment the antibacterial activity of CPs and, thus, indirectly point at the MoA involving the formation of radical oxides as the result of optically active surface and bulk defects. To that end, the optical properties of ACP and HAp were examined using UV–Vis PL and diffuse reflectance (DR) spectroscopy. The DR spectra displayed a similar adsorption edge, near 205 nm, for both ACP and HAp powders [Fig. 9(a)]. The absorption capacity of ACP in the short-wavelength UV (UVC) region (100–280 nm) was higher than that of HAp, especially at 205 nm where this capacity is almost four times higher. The higher UVC light absorption capacity of ACP may be attributed to its lower crystallinity compared to HAp. In optically inactive or weakly active materials, crystallographic defects usually present the sites of a greater optical activity compared to the points in a perfect lattice, the reason being the conformational heterogeneity of the electronic states around the defects, which causes the spread of the absorption and emission energies and makes transitions forbidden in a perfect system practically possible.[49] ACP and HAp also had a similar reflectance in the visible light region, ranging between 100% and 93.5%. Because the measurements were performed on pellets with the thickness of 1 mm, the transmission effects were neglected and the absorption capacity was directly correlated with the reflectance. The direct bandgap energies (E_{bg}) were determined from Kubelka–Munk function versus photon energy (eV) plots shown in Figs. 9(b) and 9(c) and E_{bg} values were the same, 225 eV, for both HAp and ACP. Luminescence photographs taken under the excitation of 405 nm show the brighter, bluer emission for HAp than for ACP [Figs. 9(d) and 9(e)]. This blue photoluminescence, emitting without the presence of

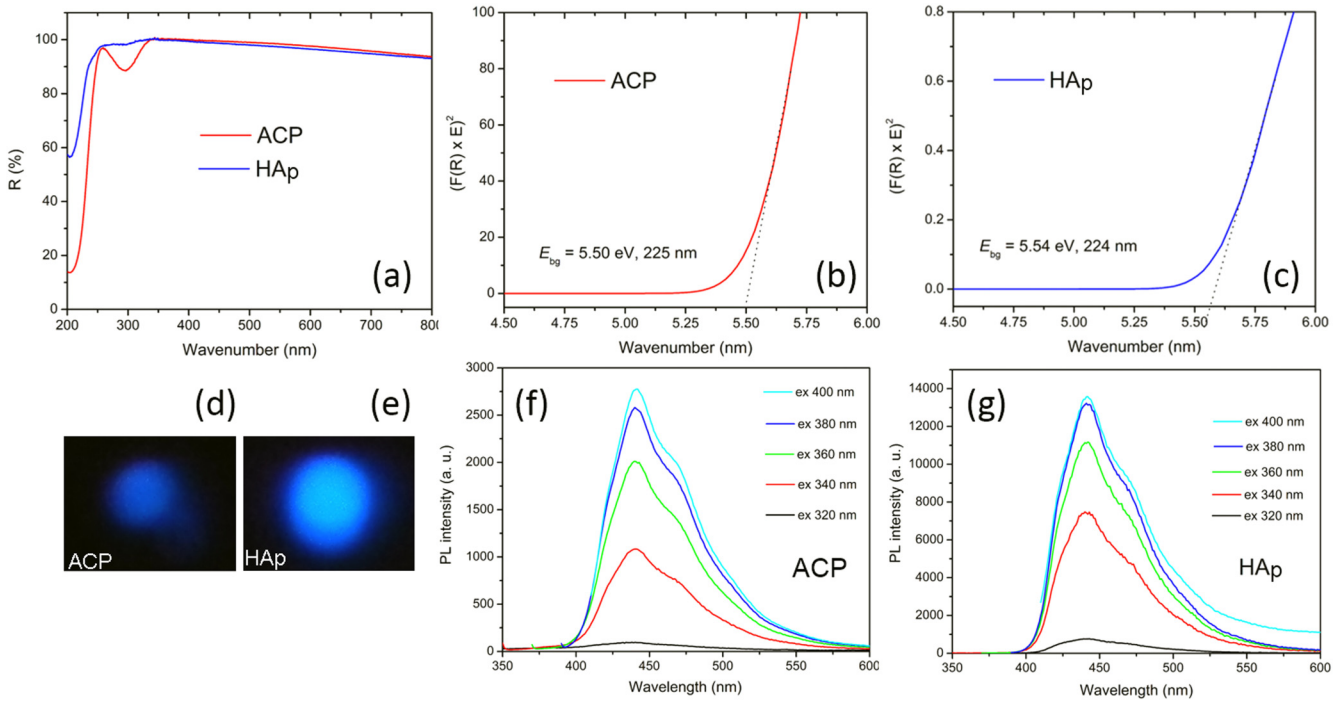

FIG. 9. UV–Vis diffuse reflectance spectra of ACP and HAp (a). Kubelka–Munk curves from which the bandgap energies for ACP and HAp were determined by extrapolation [(b) and (c)]. Luminescence photographs of ACP and HAp powders under 405 nm irradiation in the dark [(d) and (e)]. Photoluminescence spectra of ACP and HAp under different excitations [(e) and (f)].

activators, was detected before[50,51] and has a biomedical potential that extends beyond the scope of this study.[52,53] PL spectroscopy was used next to determine the type of defects present in ACP and HAp. The room temperature PL spectra are presented in Figs. 9(f) and 9(g). Although the two CP powders were sensitive to different excitation wavelengths in the 320–400 nm region, both PL spectra displayed a wide emission band in the visible, 390–600 nm range. This wide emission band was the convolution of three blue emission components centered near 440, 470, and 505 nm. These blue emission bands were caused by the surface and bulk defects, such as vacancies, structural defects, and lattice distortions. The free radical formation process is assumed to involve photo-induced formation of an electron vacancy on the particle surface and the electron transfer to a PO_4^{3-} oxygen, which is followed by the formation of a superoxide radical ($O_2^{\bullet}$) capable of oxidizing adjacent biomolecules and reacting with water molecules to produce other radicals, including hydroxyl radicals ($OH^{\bullet}$) and hydrogen peroxide (H_2O_2).[54] The higher PL intensity of HAp in comparison with that of ACP was due to a larger crystallite size and crystallinity of the former powder. The prerequisite for an efficient photocatalytic activity, such that it leads to the generation of antibacterially active species, including $OH^{\bullet}$, H_2O_2, and $O_2^{\bullet}$, is that the energy of the irradiation source lies within the bandgap of the material.[55] With the absorption by CP nanoparticles lying within the UV region, it is conceivable that the simple exposure to sunlight might be sufficient to activate the material. Namely, sunlight contains ~5%–7% of UV rays, with the rest being visible and infrared light, both present in approximately equal amounts: 46%–48%.[56]

All in all, these data indicate that a considerable concentration of defects is present on the surface and in the bulk of CP nanoparticles and that they are able to be excited in the presence of the UV radiation, endowing the particles with luminescent properties. The question, however, was whether these defects were capable of generating free radicals in contact with the solution and, thus, be responsible for the activity against bacteria. To answer this, a *P. aeruginosa* broth assay was performed with concomitant UV irradiation and the results are shown in Fig. 10. Interestingly, the reduction in the microbial population due to 5 min UV irradiation was identical to that achieved by the IC_{50} dose of ACP nanoparticles in the absence of the UV treatment. Moreover, no augmentation achieved by concomitant nanoparticle and UV treatment compared to the treatment with nanoparticles alone suggests that, though defect-generated radicals may be present in the system, they do not constitute the main MoA of these particles. This makes CP nanoparticles mechanistically different from photocatalysts such as the oxides of zinc, tin, titanium, and, to some extent, magnesium.

G. Nanoparticle diffusion coefficient

To test whether the diffusion of nanoparticles through the medium benefits their antibacterial activity, the activity of identical ACP powders was compared in broths and agar assays. As seen from Figs. 11(a) and 11(b), while 5 mg/ml of ACP powder significantly decreased the activity of *P. aeruginosa* in broths, the inhibition zones were not detected in the agar assay around 5 mg deposits of ACP powder, indicating a minimal activity of ACP under these conditions. *P. aeruginosa*, the

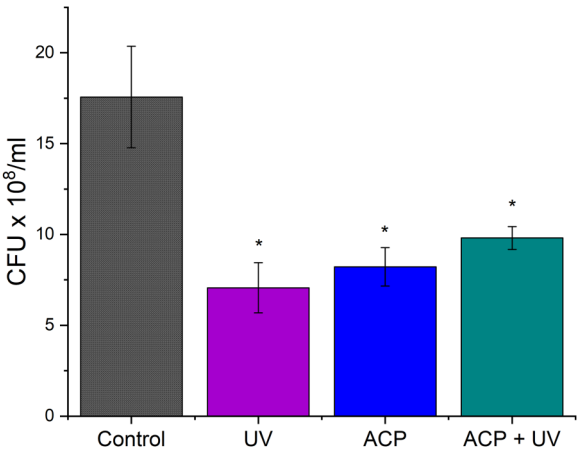

FIG. 10. Broth concentration of colony forming units of *P. aeruginosa* aged overnight after the 5 min treatment with the MIC_{50} (90 mg/ml) of ACP with (ACP + UV) and without (ACP) the concomitant UV irradiation compared to the broths treated with UV light alone (UV) and broths not subjected to any treatment (control). Data points represent averages (n = 3) and error bars represent the standard deviation. Data points statistically significantly lower ($p < 0.05$) compared to the control, untreated population are marked with an asterisk.

specie selected for this assay, was not observed to form any more biofilm on agars than in broths, where the biofilm amount forming was considerable. Similar results were, however, obtained for a nonbiofilm-forming species, *E. coli*. Agar assays were also performed to compare the activity of ACP powders and their corresponding viscous suspensions against *P. aeruginosa*. As can be seen from Figs. 11(b) and 11(c), whereas ACP powder displayed no inhibition zone around it, these zones were pronounced against ACP gels. As viscous gels diffuse into the infected agars more pronouncedly than the powders, this difference in the effect between the two formulations suggests that the activity of CPs is critically dependent on the ability of the nanoparticles to diffuse to the bacterial cell as opposed to acting as a static substrate that sits and waits for the bacteria to bind to it. An earlier study showed a negligible antibacterial effect of ACP nanoparticles with a similar size (116 nm on average) as those utilized in this study, but brought into contact with bacteria in the compact form, as composite blocks.[57] The fact that the antibacterial effect is present when ACP nanoparticles are delivered as powders suggests that their diffusion through the medium is one of the prerequisites for

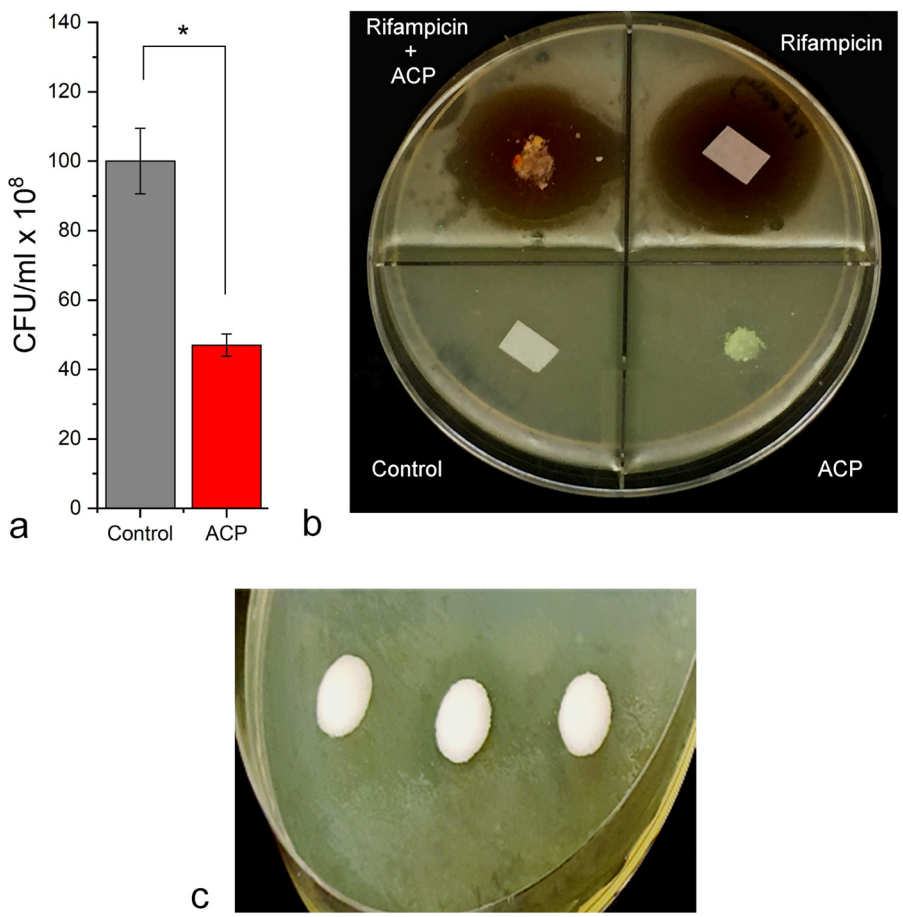

FIG. 11. Reduction in the broth concentration of colony forming units of *P. aeruginosa* after the treatment with 5 mg/ml of ACP powder compared to the untreated, negative control (a). No inhibition zone forming around 5 mg of ACP powder deposited on an agar plate inoculated with *P. aeruginosa* and distinct zones of inhibition forming around rifampicin and rifampicin-loaded ACP (b). Moderate zones of inhibition forming around 5 mg of ACP cements deposited on an agar plate inoculated with *P. aeruginosa* (c).

their action. Since most clinical applications of CPs utilize it as a static materials component, be it as bioactive coatings of implants or to reinforce tissue engineering constructs, these insights suggest that the benefits of the diffusive form of the same nanoparticles might be even greater, albeit being greatly unexplored. These experiments are in agreement with the higher activity of nanoparticles than that of the larger particulates that was elaborated earlier in the text. However, they also hint at the significant role played in the process by even finer atomic clusters, which we cover in Sec. III H.

H. Ion/cluster exchange dynamics across the particle/solution interface

CP particles exhibited the antibacterial effect in both the pulverized and the cement form, with a clear difference in the particle size between the two (Sec. III D). Although the bacteria were consistently less viable when challenged with the formulations containing lower particle sizes, the difference was statistically significant only in one-third of all comparisons, and both formulations were capable of significantly inhibiting the bacterial growth [Fig. 7(c)]. This has suggested that the nanosize of primary CP particles plays an important role, but is not the major antibacterial factor.

CP particles are typified by an extraordinary phase composition volatility and dynamics at the interface with aqueous solutions. The inherent instability of CP particles predisposes them for a constant exchange of ions and fine atomic units, comparable in size to $Ca_9(PO_4)_6$ hexagons aka Posner's clusters, across the solid/liquid interface, regardless of the particle size. The formation of HAp, for example, proceeds through hierarchical aggregation of differently sized growth units, with the finest of them being 9 Å sized Posner's clusters. Although this aggregation-based growth is usually associated with biomimetic, surface-controlled precipitation,[58,59] it is also observed as the mechanism of growth in the absence of any organic additives.[60–62] In addition, an equilibrium state at the solid/liquid interface implies a finite exchange of ions between the two phases and this exchange is expected to be more intense in HAp than in other oxides because of its intrinsically hydroxylated nature. As a result, these clusters are expected to constantly surround CP particles in contact with the aqueous medium, even when preformed particles are dispersed in it. Visualizing these ultrafine, transient entities would require the stretching of the spatiotemporal resolution of state-of-the-art aberration-corrected transmission electron microscopes beyond their current limits and more indirect analytical techniques must be resorted to. A couple of experiments based on these techniques were designed to test the effect of the cluster exchange dynamics across the particle/solution interface, imaginable as the tail of a comet as it traverses the cosmic space. In conceiving the first experiment, we were guided by the idea that ACP should create a higher concentration of these units within the Stern layer and Debye length limits than crystalline apatite.

The greater degree of exchange of content across the particle/solution interface in ACP compared to its crystalline counterpart, HAp, was indirectly illustrated by a higher release rate of three different molecules from ACP than from HAp [Figs. 12(a)–12(c)]. These molecules included a large protein, bovine serum albumin (BSA), and two small molecules with almost identical molecular weights but with a very different hydrophobicity: a model drug, fluorescein (log P = 3.2), and an antibiotic, ciprofloxacin (log P = −1.4). Fluorescein was released faster than BSA and BSA was released faster than ciprofloxacin, showing that the retention of the compound on the particle surface is directly proportional to the hydrophilicity of the compound. The release efficiency measured on ACP and HAp for three different antibiotics, including ampicillin, vancomycin, and erythromycin, confirmed that all three drugs, irrespective of their chemical properties, adsorb on and desorb from ACP much more efficiently than from HAp [Figs. 12(d)–12(f)], presumably because of a greater degree of content exchange across the particle/solution interface in ACP. These results also demonstrate that small hydrophobic molecules (e.g., fluorescein or ampicillin) adsorb on and desorb from highly convex nanoparticle surfaces better than large hydrophilic molecules (e.g., BSA or vancomycin). Hence, the amount of the drug loaded onto the particles and released within 24 h when normalized to the weight of the carrier was highest for ampicillin (logP = 0.9, M_w = 349.4 g/mol), reaching 400% for ACP, which was higher than 70% and 4.8% for vancomycin (logP = −3.1, M_w = 1449.3 g/mol) and erythromycin (logP = 3.1, M_w = 733.9 g/mol), respectively [Figs. 12(d)–12(f)]. The same trend was observed for HAp, with the most efficiently loaded and released drug being ampicillin (146%), ahead of vancomycin (15.2%) and erythromycin (3.5%), confirming that large size is a greater hindrance to adsorption onto CP nanoparticles than hydrophobicity. Since drugs are loaded onto CP nanoparticles strictly via adsorption, the release rate should be directly proportional to the fluctuant flux of ions and clusters across the solid/liquid interface. The greater lattice disorder, higher hydration, and lower enthalpy allow for bond breaking at a lower energetic cost on the surface of ACP, leading to a greater surface dynamics and, consequently, faster desorption of molecules.

The idea that the entities alternately dissipating from and reintegrating with the particle surface exhibit a critical effect on the antibacterial activity of CP nanoparticles was also tied to our rejection of the simple interfacial free energy argument. Namely, lower hydration on the surface of HAp and its lower degree of entropic similarity with the medium imply a higher interfacial free energy compared to ACP. Given its higher interfacial free energy compared to ACP, HAp would present the site of a greater attraction to proteins, which it could potentially destabilize. However, although HAp was indeed more toxic to MDR strains, this could not explain that ACP was more toxic to Gram-positive lab strains. Hence, we were prompted to search for the key to explaining this selective activity in a greater structural and stoichiometric instability and dissipative composition of ACP, notwithstanding that HAp also must have a unique or very pronounced structural feature that endows it with a

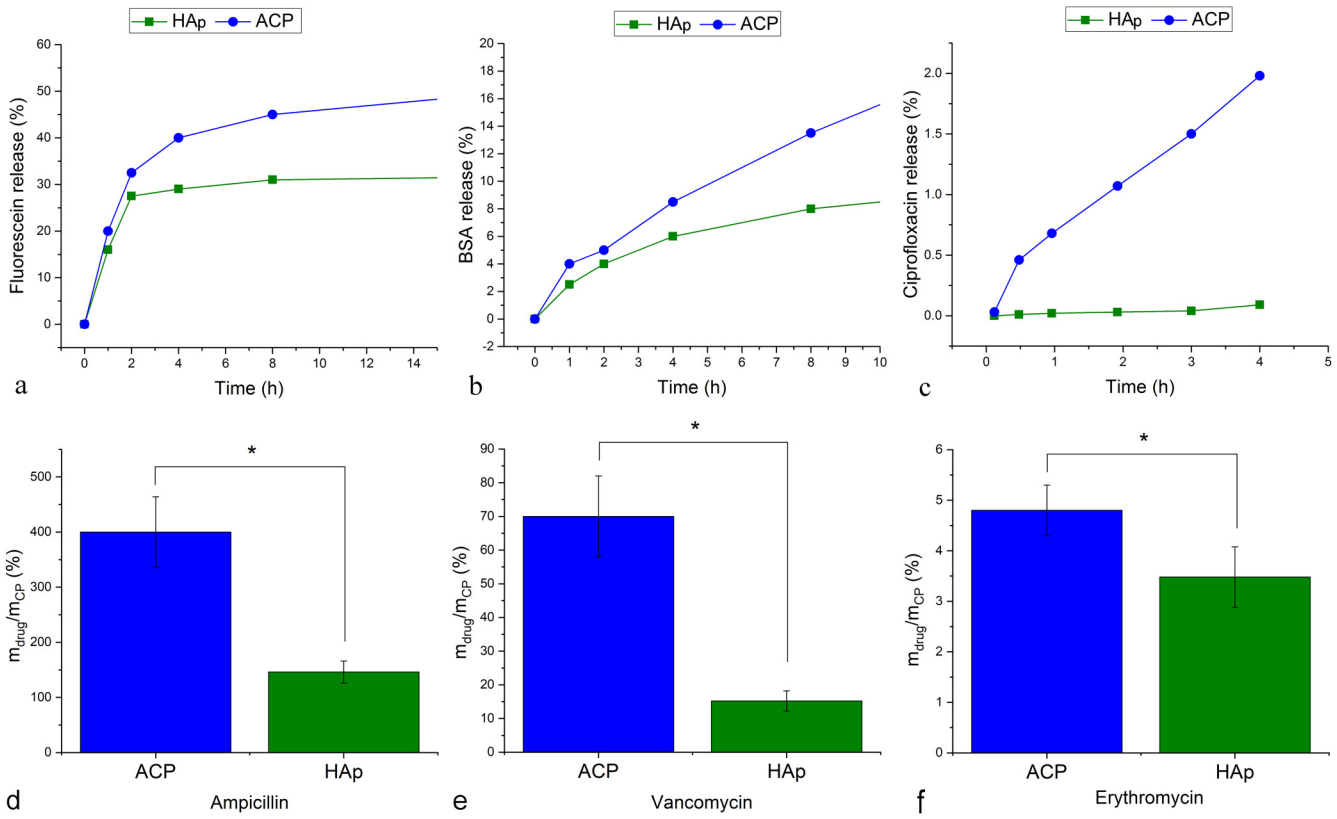

FIG. 12. Kinetic profiles for three different molecules—fluorescein (a), bovine serum albumin (b), and ciprofloxacin (c)—released from HAp or ACP powders [(a) and (b)] or gels (c). The amounts of three different antibiotics—ampicillin (d), vancomycin (e), and erythromycin (f)—loaded and released within 24 h from ACP and HAp and normalized to the weight of ACP/HAp.

potential to surpass the activity of ACP against certain bacterial species.

Compared to its more stable compositional analogue, HAp, we envisaged ACP as a nanoscopic comet leaving a greater trail in a biological milieu, generating fine clusters that may be toxic to bacteria. These dynamic changes present at the particle/solution interface are enabled by the intensely hydrated and diffusive apatitic surfaces in general,[63,64] but should be more intense for an amorphous state, which is by definition metastable and prone to change toward more thermodynamically stable states. If validated, this hypothesis could explain a significant amorphous content of biomineral in bone[65] and tie it not only to the remodeling process, but also to the provision of an intrinsic prophylactic activity to bone against the bacterial proliferation. One such model of antibacterial activity would be conditioned by the validity of the assumption that phase transitions from as-precipitated ACP to crystalline HAp proceed at least partially through the dissolution/reprecipitation mechanism. Many are reported physical effects indicating the correctness of this mechanism, including the inhibition of the growth of HAp from ACP after polymers were adsorbed onto ACP surface,[66] the preservation of ACP structure by interspersing ACP particles inside a chitosan matrix,[67] and the increased rate of HAp nucleation and ACP → HAp transformation at a lower pH,[68] when the dissolution of ACP is increased. The idea about the disparity between the dynamics of the unceasing transition between the solution and the crystal on the surface of ACP and HAp is reflected in the conditions under which these two solids form: while both ACP and HAp initially form as amorphous phases,[69] prolonged metastability of ACP is ensured by the more dynamic conditions of precipitation, involving abrupt mixing of reagents and a rapid attainment of sufficiently high supersaturation levels,[70] thus favoring spontaneous precipitation of constitutive ions.[71] In contrast, the transition of as-precipitated ACP to HAp is fostered at lower supersaturations and in processes involving heterogeneous nucleation on organic and other hydrophilic substrates.[72]

As the transformation of the powder into cement increases the amorphous content in the material, this would increase the cometlike tail that the particles create in their diffusion wake. This effect would be partly due to the greater degree of amorphousness in the wet cements, but also partly due to the pasty, heavily hydrated and semifluid character that the material adopts in such a form. To that end, we compared the antibacterial efficacies of dry powders and wet, not dry cements as in the earlier experiment [Fig. 7(c)] as well as the efficacies of dry and wet cements. The experiment comparing wet versus dry cements, assuming that the former would have a greater concentration of Posner's clusters and other fine particulate units moving back and forth across the solid/liquid interface, has shown that the wet cements significantly increase the antibacterial activity. Thus, whereas the treatment of *E. coli* broths with 10 mg/ml of dried HAp cements

decreased the bacterial colony count compared to the untreated control, albeit not in a statistically significant manner, the treatment with wet HAp cements did so with a confident level of statistical significance [Fig. 13(a)]. In contrast, ACP cements did not produce a difference in bacterial concentrations depending on whether they were delivered as wet or dried, presumably because ACP *per se* contains a rich solid/liquid interface thanks to its amorphous character, which becomes barely increasable when the hydration of the material is changed. One such change, expectedly, produces a more significant effect in HAp, a CP phase more deprived of this rich interface in its dry, crystalline state compared to ACP.

The second experiment involved aging fresh HAp precipitates in the parent solution for various periods of time and also subjecting half of the samples in each sample group to a thermal treatment by bringing the suspensions to boil. The premise was that both aging and heating should stabilize the nanoparticle surface by increasing the crystalline order and reducing hydration. The fact that the HAp precipitate heated and aged for the longest period of time exhibited a higher antibacterial activity than precipitates with an identical phase composition, but aged for shorter periods of time and not heated [Fig. 13(b)] suggests that particle properties becoming less prominent following such treatments are not responsible for exhibiting the antibacterial effects. These properties include those dependent not only on surface defects but also on the dynamics of the interfacial processes involving Posner's clusters and ionic species alternately separating from and anchoring back to the particle surface, all of which should decrease in abundance with the aging and thermal treatments. This observation is corroborated by no difference between *P. aeruginosa* populations in broths treated with HAp/ACP powders, which are relatively impoverished in the content of Posner's clusters, and broths treated

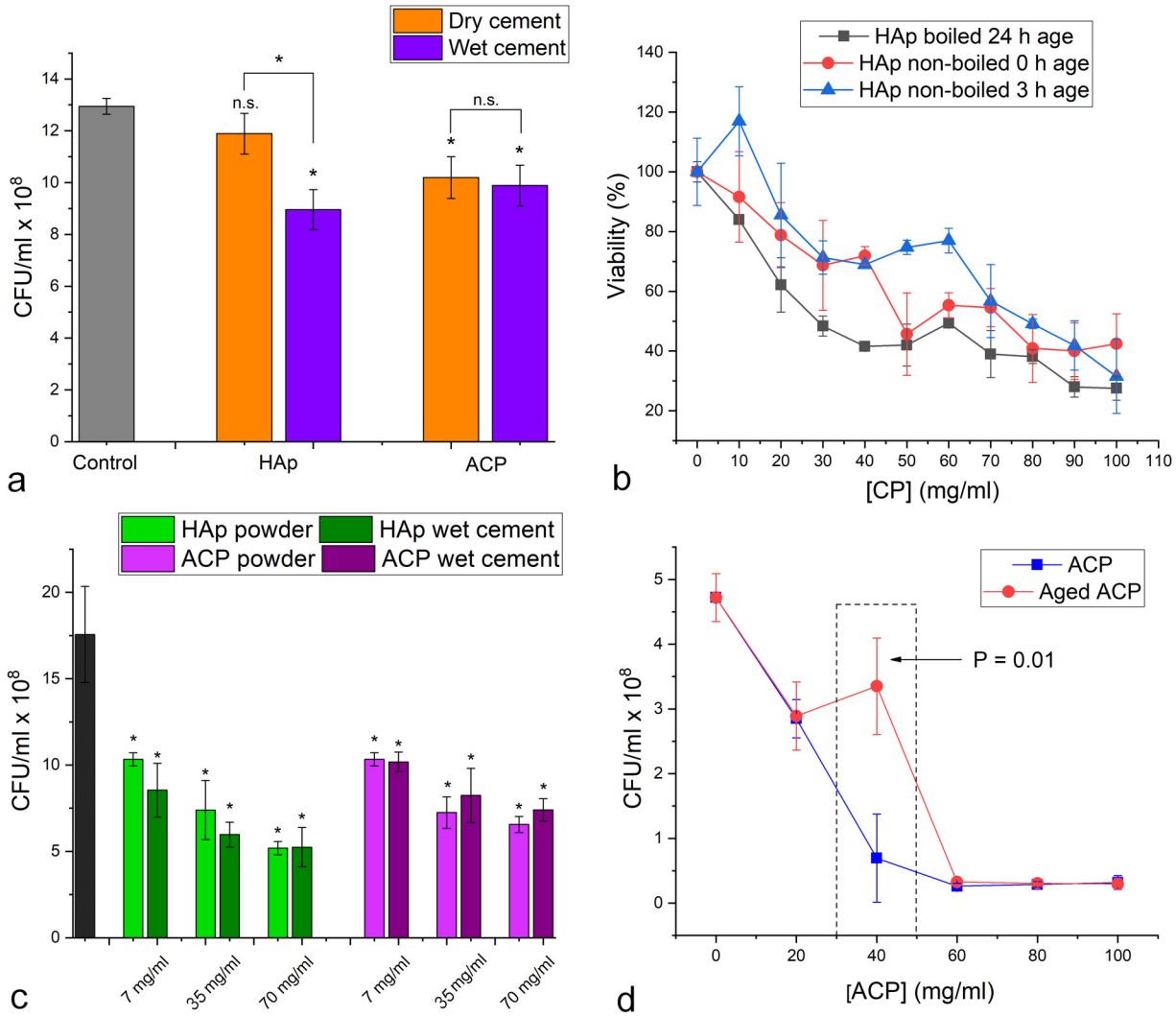

FIG. 13. Comparison in the reduction of the concentration of colony forming units in *E. coli* [(a), (b), and (d)] or *P. aeruginosa* (c) bacterial broths treated with different concentrations of 10 mg/ml HAp or ACP nanoparticles delivered as wet or dried cements (a), HAp nanoparticles prepared with and without the boiling step and involving different precipitate aging times in the solution (b), HAp or ACP nanoparticles delivered as powders or as wet cements (c), and ACP nanoparticles either freshly precipitated or aged in the solution for 3 h (d). Data points represent averages ($n = 3$) and error bars represent the standard deviation. Data points statistically significantly lower ($p < 0.05$) compared to the control, untreated population are marked with an asterisk.

with the comparative concentrations of the same particulates delivered as wet cements, presumably relatively richer in the content of Posner's clusters [Fig. 13(c)]. Another confirmation of little to no effect of the cluster exchange dynamics came from an experiment comparing the antibacterial activity of fresh and aged ACP powders. ACP precipitate is expected to solidify structurally as its aging time in the parent solution is increased; however, the nonexistent difference between *E. coli* colony count in broths challenged with fresh ACP and in broths challenged with aged ACP [Fig. 13(d)] supports the idea that Posner's clusters are not a significant antibacterial factor. That they may exert some effect, however, can be concluded from the higher activity of the fresh and Posner-cluster-enriched ACP than its aged counterpart at 40 mg/ml dose [Fig. 13(d)]. All of this suggests that these clusters, alongside other transient species consequential to the interfacial dynamics, do play some, but not the major role in causing the antibacterial activity of CPs.

I. Particle morphology effects

For the sake of curiosity, the note on which science should begin and end, we analyzed the effect of the sequence of the addition of reagents during synthesis on antibacterial properties of the powder product. Thus, we compared particles precipitated by introducing Ca^{2+} ions dropwise to a phosphate-rich solution with the regular precipitates prepared in the opposite manner, that is, by adding $H_xPO_4^{x-3}$ ions dropwise to a calcium-rich solution. Variations in the sequence of addition of reagents to a mixture have routinely caused changes in materials properties, including particle size and specific surface area, in turn, affecting their performance.[73] In our case, this variation produced no significant change in the particle size, but it caused a minor, but detectable level of change in the particle morphology: namely, HAp nanoparticles precipitated at low Ca/P ratios, by adding Ca^{2+} ions to a phosphate-rich solution, had somewhat sharper edges [Fig. 14(b)] than HAp nanoparticles precipitated at high Ca/P ratios [Fig. 14(a)]. This difference is expected in view of the fact that precipitation at a high concentration of the more chaotropic ion, in this Ca^{2+}, is performed when one wants to break the crystalline symmetry and produce round morphologies. In contrast, precipitation at a high concentration of the more kosmotropic ion, in this PO_4^{3-}, is performed when one wants to conduct crystal growth in conformity with the crystalline symmetry of the compound and produce more complex morphologies. Biomimetic precipitation of apatite proceeds at a low Ca/P molar ratio,[74] presumably because the phosphate network provides a heavier, kosmotropic ionic skeleton to be filled with the lighter, more diffusive and chaotropic Ca^{2+} ions. This precipitation results in elongated, plate-shaped morphologies[75] that conform to the hexagonal space group of HAp and is also in agreement with the more decisive effect of anions on the microarchitecture of fine particles[76] and with the order-breaking effect Ca^{2+} ions impose on many biological structures.[77] Also, it should be noted that even in the absence of an evident change in particle properties due to a variation of the sequence of the addition of reactants to the mixture, a change in the surface composition and double layer dynamics caused by this procedural variation could have a powerful influence on the particle/cell interaction.

The difference in the antibacterial activity depending on the sequence of reagent addition was noticeable and very pronounced against *E. coli*, in which case the HAp powder prepared at low Ca/P ratios was more effective than the powder prepared at high Ca/P ratios at all three tested

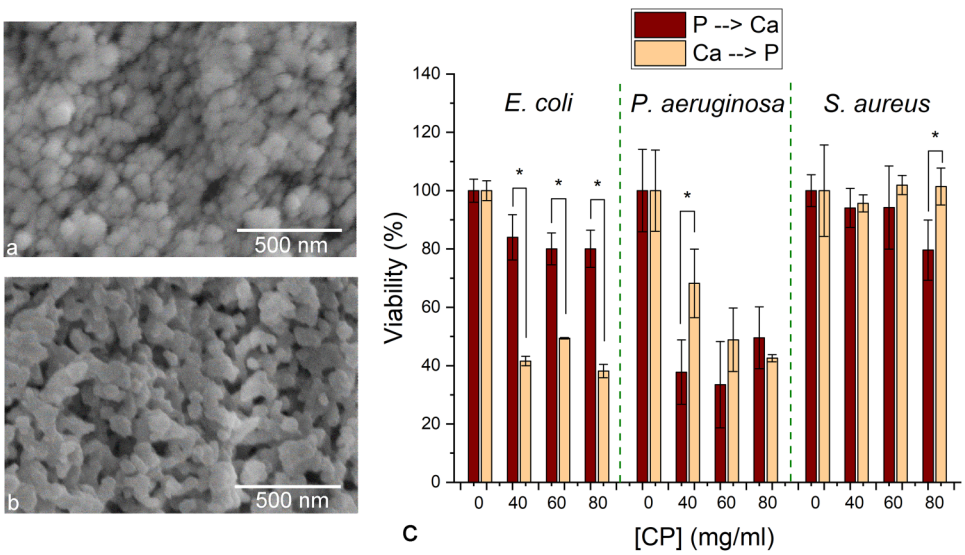

FIG. 14. SEM images of HAp nanoparticles synthesized by the addition of an $NH_4H_2PO_4$ solution into a $Ca(NO_3)_2$ solution (P → Ca) (a) or by the addition of a $Ca(NO_3)_2$ solution into an $NH_4H_2PO_4$ solution (Ca → P) (b). Viability reduction of different bacterial populations, including *E. coli*, *P. aeruginosa*, and *S. aureus*, in response to the treatment of HAp nanoparticles in doses of 0, 40, 60, and 80 mg/ml depending on whether they were formed by introducing an $NH_4H_2PO_4$ solution into a $Ca(NO_3)_2$ solution (P → Ca) or *vice versa* (Ca → P) (c). Data points represent averages (n = 3) and error bars represent the standard deviation. Data points statistically significantly different ($p < 0.05$) with respect to the comparative data point are marked with an asterisk.

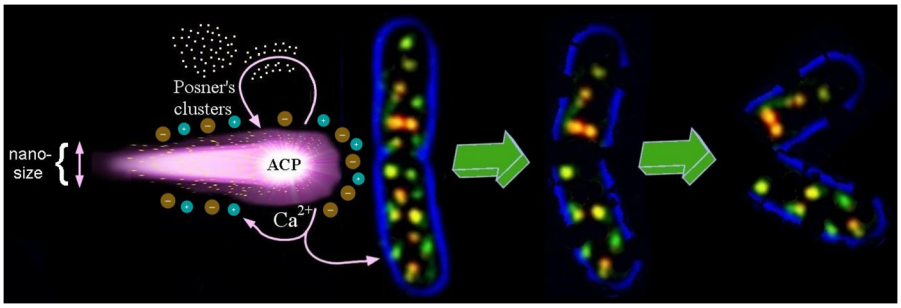

FIG. 15. Scheme describing key particle properties acting as determinants of the antibacterial activity of CP nanoparticles in interaction with bacterial cells, including (a) nanoscopic size; (b) release of calcium ions and elevation of the intracellular concentration of calcium; (c) diffusivity and low globally negative charge of a zwitterionic surface that minimizes the electrostatic barrier posed before the nanoparticle approaching the bacterial cell; and (d) Posner's and similarly sized atomic clusters creating a rich and dynamic hydrodynamic environment surrounding the diffusive nanoparticles, analogous to the tail of a comet, constantly dissipating and reintegrating with the particle surface, the drawing of the limits of which is challenging because of the complexity of this interface.

concentrations. A significant difference between the activities of the two powders against *P. aeruginosa* was present only at the lowest of the three particle concentrations tested and in that case, the opposite effect from that observed in *E. coli* was at work [Fig. 14(c)]. Similarly, the activity of the powder prepared at high Ca/P ratios was higher in *S. aureus*, albeit only at the highest concentration in a significant manner [Fig. 14(c)]. The fact that the antibacterial effect against *E. coli* was more pronounced for the somewhat sharper particles of HAp precipitated at low Ca/P ratios—that is, when Ca^{2+} was added to $H_xPO_4^{x-3}$ rather than vice versa—may suggest that elongated and other anisotropic particle morphologies may be often, but not always, more toxic to the cells than their rounder counterparts. This insight would be drawn in analogy to the shape effect observed in calcified deposits in atherosclerotic plaque,[78] asbestos in lung disease,[79] and filamentous bacteria that are less efficiently phagocytosed than bacilli or cocci.[80] Our previous study demonstrated that rounder CP particle morphologies translate to a greater antimicrobial potency, but only when sizes of these particles are lower than those of their plate- and needle-shaped analogues.[81] As we show here, if the particle size remains unchanged, particles with sharper edges may be deadlier to some bacteria than their rounder counterparts. Also, with the antibacterial effect against *E. coli* being more intense for the powder prepared at low Ca/P ratios, this may indirectly reiterate the abovementioned point that diffusive ionic units on the particle/solution interface, which should be more concentrated in this material, are a factor defining the antibacterial activity of these CPs. Overall, experiments involving a variation to the reagent addition sequence illustrates a fine point, which is that the antibacterial activity of CPs can be controlled and optimized within a broad window of values by relatively simple means. It brings hope that with a sufficient input of materials chemistry knowledge, the antibacterial activity of CPs could be made competitive with the more popular and applied inorganic alternatives. This hope will be the driver of the future optimization studies.

IV. CONCLUSION

In the first part of this study,[1] we evidenced and elaborated on a definite antibacterial effect of two different CPs, namely, HAp and ACP, both alone and in synergy with antibiotics. A number of antibiotics ineffective against particular bacterial species were suddenly rendered effective when they were codelivered with CP nanoparticles. There was also a selective effect depending on the crystallinity of CPs, with the most drastic example being that of Gram-positive species, against which ACP was active and HAp was not. Also, while HAp was ineffective against regular Gram-positive species, it proved effective against their MDR analogues. In this, second part of the study, we engaged in the quest for a key CP nanoparticle property responsible for eliciting these curious effects. A number of material properties were subjected to systematic scrutiny and some of them were discarded as nonessential for explaining the antibacterial effect, thus putting an end to frequently erred hypotheses in the literature. For example, while both HAp and ACP displayed blue emission bands owing to crystallographic defects, these defects were incapable of generating reactive oxygen species under excitation in concentrations sufficient to induce bacteriostasis and it was concluded that CPs do not share the photocatalytic MoA with materials such as ZnO or TiO_2.

A few properties of CP particles stood out as having a definite, albeit not decisive effect on their antibacterial activity. These effects are graphically depicted in Fig. 15. First, the nanosized nature of the particles is highlighted because it presented a prerequisite for their exhibition of the antibacterial mode of action. Second, the ability of the nanoparticles to move through the medium and diffuse their way to the cell was essential too. The zwitterionic nature of the nanoparticle surface and its globally negative charge, albeit relatively low in magnitude, was hypothesized to have played a role in minimizing the electrostatic repulsion barrier between the nanoparticle and the cell and facilitating their coming into contact with one another, if not providing the electrostatic attraction to cationic residues of the peptidoglycans and polysaccharides covering the surface of Gram-positive and Gram-negative bacteria, respectively. Finally, there was the benefit of the particles' rich interface exchange dynamics, through which they form a cometlike tail by continuously dissipating and reintegrating their content in the form of fine atomic clusters as they move through the liquid

medium. Coming into contact with the peptidoglycans of the cell wall, these fine clusters do not redeposit on the CP particle surface, effectively in a constant state of recrystallization, but are able to interfere with and disrupt the structure of these biological entities. A portion of this ionic trail permanently leaves the particles and may affect the bacteria if exceeding particular thresholds, which brings us to the fourth effect, namely, bacteria challenged with CP nanoparticles contained twice more intracellular Ca^{2+} ions than the control bacteria. Most of these numbered effects are affected by crystallinity, thus explaining the fundamental disparity between the effect of ACP and HAp on Gram-positive species. None of these effects, however, was of such a critical magnitude that it could be a major or sole determinant of the antibacterial activity. Also, given that there are multiple properties of importance, it would be erroneous to exclude the effects of properties that had no effect in the assays we designed here because they might be just as well tying the aforementioned properties together. Generation of nanopockets rich in protons upon reprecipitation of surface units dissipated in action and the hydrodynamic cloud enriched in Ca^{2+} ions surrounding the particle as the result of this alternate dissolution and crystallization may be such phenomena that alone have no effect on the bacteria, but are essential components of a complex synergy of factors. One of these inactive factors might be crucial in facilitating the transport of active factors to the site of action. For example, even if Ca^{2+} ions generated by the dissolution of the fine CP clusters forming due to the dissolution/recrystallization processes going on continuously on the particle surface may not be capable of distorting the native structure and function of the biomolecules that they come in contact with and induce downstream effects causative of necrosis and other toxic responses in the host cells, they may still act as Trojan horses opening up porins, pumps, or ion channels and enabling the intracellular passage of the nanoparticles. As it frequently happens, in search of an answer to a question, we have come across ever more complex questions. Explaining this intricate synergy presents an enigma that confirms the age-old adage, according to which "every answer asks a more beautiful question."[82] The failed quest for a holy grail, a philosopher's stone that a single key parameter represents may be disappointing to some, but not to anyone familiar with the complex machinery called life where operations proceed along redundant feedback loops that distribute the regulatory role over multiple nodes of the network and ensure that the failure of any single one of them does not affect the workings of the whole.

The synergistic effect of multiple particle properties, emerging from the partial effect found in a number of hypothesized mechanisms, is in agreement with the general nature of inorganic antibacterial materials, including their role model, silver.[83] This multifaceted mechanism is also a natural corollary of the pleiotropic nature of CPs. On the positive note, to this mechanistic pleiotropy and nonspecificity CP nanoparticles owe their lesser potential to cause resistance to therapy typical of narrow-range target-specific molecular antibiotics. On a fundamentally problematic side, the fact that a synergy of multiple factors is responsible for causing the antibacterial effect implies an extraordinary difficulty of elucidating the MoA, the fate of which may be common to ceramic materials in general. On yet another, more practically problematic side, this synergetic combination of causes of the antibacterial activity of CPs makes the rational design of theirs for this type of medical application difficult, but not impossible. If synergetic, the exploration of the MoA is inevitably multifactorial and may take an infinite number of possible angles, depending on their combinations and contexts in which the studies would be conducted. Hence, the search is far from over. Even now when the key particle properties are delineated, a long and tortuous path leads through particle design and property optimization in search of clinically relevant efficacies. If it took 14 years from the discovery of penicillin for its structure to be determined, 16 for its mass production method to be reported and 29 for it to be chemically synthesized, nothing short of an equally winding path from the bench to the bedside can be expected in this case too. In the end, we hope that the versatile, pleiotropic nature of CPs complies with this multifaceted mechanism and will be advantageous in the long run, not only because the microbiome transitioning endogenously from the opportunistic to the pathogenic is polymicrobial by nature, but also because this intrinsic versatility and tunability can be the gateway to the sphere of personalized medicine toward which the most advanced biomaterial therapies stream.

CONTRIBUTIONS

V.M.W. was involved in data acquisition, formal analysis, investigation, methodology, and supervision. S.T. was involved in data acquisition. M.G.N. and S.M. were involved in data acquisition for Sec. III F and formal analysis for Sec. III F. V.U. was involved in formal analysis, funding acquisition, investigation, methodology, resources, supervision, and writing.

ACKNOWLEDGMENT

The National Institutes of Health grant (No. R00-DE021416) is acknowledged for support.

[1]V. M. Wu, S. Tang, and V. Uskoković, ACS Appl. Mater.Interfaces **10**, 34013 (2018).
[2]C. N. Rochette, S. Rosenfeldt, A. Heiss, T. Narayanan, M. Ballauff, and W. Jahnen-Dechent, ChemBioChem **10**, 735 (2009).
[3]L. C. Pele *et al.*, Nanomed. Nanotechnol. Biol. Med. **13**, 619 (2017).
[4]J. J. Powell *et al.*, Nat. Nanotechnol. **10**, 361 (2015).
[5]C. Llena, L. Forner, and P. Baca, J. Contemp. Dent. Pract. **10**, 1 (2009).
[6]R. K. Rose, Caries Res. **34**, 427 (2000).
[7]B. Ingham, G. D. Erlangga, A. Smialowska, N. M. Kirby, C. Wang, L. Matia-Merino, R. G. Haverkamp, and A. J. Carr, Soft Matter. **11**, 2723 (2015).
[8]J. Zhao, Y. Liu, W.-B. Sun, and H. Zhang, Chem. Cent. J. **5**, 40 (2011).
[9]A. Azarpazhooh and H. Limeback, J. Am. Dent. Assoc. **139**, 915 (2008).
[10]C. Rahiotis, G. Vougiouklakis, and G. Eliades, J. Dent. **36**, 272 (2008).
[11]G. K. Divyapriya, P. C. Yavagal, and D. J. Veeresh, Int. J. Oral Health Sci. **6**, 18 (2016).
[12]C. Chen, M. D. Weir, L. Cheng, N. J. Lin, S. Lin-Gibson, L. C. Chow, X. Zhou, and H. H. Xu, Dent Mater. **30**, 891 (2014).

[13]E. L. Pearce, E. M. Hancock, and I. H. Gallagher, Arch. Oral Biol. **29**, 521 (1984).
[14]J. Tanaka, N. Mukai, M. Tanaka, and M. Tanaka, Int. J. Dent. **2012**, 452108.
[15]S. Lemaire, F. Van Bambeke, D. Pierard, P. C. Appelbaum, and P. M. Tulkens, Clin. Infect. Dis. **52**, S493 (2011).
[16]L.-W. Du *et al.*, Cryst. Growth Des. **13**, 3103 (2013).
[17]R. A. Hirst, C. Harrison, K. Hirota, and D. G. Lambert, "Measurement of [Ca^{2+}]i in whole cell suspensions using fura-2," in *Methods in Molecular Biology, Vol. 312: Calcium Signaling Protocols*, 2nd ed., edited by D. G. Lambert (Humana, Totowa, NJ, 2005).
[18]P. D. Bragg and D. J. Rainnie, Can. J. Microbiol. **20**, 883 (1974).
[19]Q. L. Feng, J. Wu, G. Q. Chen, F. Z. Cui, T. M. Kim, and J. O. Kim, J. Biomed. Mater. Res. **52**, 662 (2000).
[20]M. Yamanaka, K. Hara, and J. Kudo, Appl. Environ. Microbiol. **71**, 7589 (2005).
[21]R. Meena, K. Kesari, M. Rani, and R. Paulraj, J. Nanoparticle Res. **14**, 1 (2012).
[22]A. E. Ewence, M. Bootman, H. L. Roderick, J. N. Skepper, G. McCarthy, M. Epple, M. Neumann, C. M. Shanahan, and D. Proudfoot, Circ. Res. **103**, e28 (2008).
[23]S. V. Dorozhkin, J. Funct. Biomater. **4**, 209 (2013).
[24]K. J. Thomas III and C. V. Rice, Biometals **27**, 1361 (2014).
[25]Y. Xie and L. Yang, Sci. Rep. **6**, 20628 (2016).
[26]J. E. Baik, K. Y. Kum, C. H. Yun, J. K. Lee, K. Lee, K. K. Kim, and S. H. Han, J. Endod. **34**, 1355 (2008).
[27]D. Aderka, D. Schwartz, M. Dan, and Y. Levo, Arch. Intern. Med. **147**, 232 (1987).
[28]V. Uskoković and T. A. Desai, J. Biomed. Mater. Res. Part A **101**, 1416 (2013).
[29]P. Gangola and B. P. Rosen, J. Biol. Chem. **262**, 12570 (1987).
[30]F. Betts, N. C. Blumenthal, A. S. Posner, G. L. Becker, and A. L. Lehninger, Proc. Natl. Acad. Sci. U.S.A. **72**, 2088 (1975).
[31]R. Naseem, I. B. Holland, A. Jacq, K. T. Wann, and A. K. Campbell, Biochim. Biophys. Acta Biomembr. **1778**, 1415 (2008).
[32]M. Grodzik, E. Sawosz, M. Wierzbicki, P. Orlowski, A. Hotowy, T. Niemiec, M. Szmidt, K. Mitura, and A. Chwalibog, Int. J. Nanomed. **6**, 3041 (2011).
[33]C. A. Orme and J. L. Giocondi, "The use of scanning probe microscopy to investigate crystal-fluid interfaces," in *Perspectives on Inorganic, Organic, and Biological Crystal Growth from Fundamentals to Applications*, edited by M. Skowronski, J. J. DeYoreo, and C. A. Wang (American Institute of Physics, Melville, NY, 2007).
[34]A. Carino, C. Ludwig, A. Cervellino, E. Müller, and A. Testino, Acta Biomater. **74**, 478 (2018).
[35]D. I. Andresson, D. Hughes, and J. Z. Kubicek-Sutherland, Drug Resist. Updates **26**, 43 (2016).
[36]A. M. Carmona-Ribeiro and L. D. de Melo Carrasco, Int. J. Mol. Sci. **14**, 9906 (2013).
[37]X. L. Fan *et al.*, ACS Appl. Mater. Interfaces **10**, 10428 (2018).
[38]S. Jiang and Z. Cao, Adv. Mater. **22**, 920 (2010).
[39]M. He *et al.*, Acta Biomater. **40**, 142 (2016).
[40]V. Uskoković and T. A. Desai, ACS Appl. Mater.Interfaces **6**, 13209 (2014).
[41]V. Uskoković, Z. Castiglione, P. Cubas, L. Zhu, W. Li, and S. Habelitz, J. Den. Res. **89**, 149 (2010).
[42]L. Gritsch, C. Lovell, W. H. Goldmann, and A. R. Boccaccini, J. Mater. Sci. Mater. Med. **29**, 18 (2018).
[43]L. Tronstad, J. O. Andreasen, G. Hasselgren, L. Kristerson, and I. Riis, J. Endod. **7**, 17 (1981).
[44]V. Uskoković, J. Biomed. Nanotechnol. **9**, 1441 (2013).
[45]S. Hirn *et al.*, Eur. J. Pharm. Biopharm. **77**, 407 (2011).
[46]J. R. Morones, J. L. Elechiguerra, A. Camacho, K. Holt, J. B. Kouri, and J. T. Ramirez, Nanotechnology **16**, 2346 (2005).
[47]L. S. Taylor and G. G. Z. Zhang, Adv. Drug Deliv. Rev. **101**, 122 (2016).
[48]P. J. ter Brugger, J. G. Wolke, and J. A. Jansen, J. Biomed. Mater. Res. **60**, 70 (2002).
[49]E. Vella, F. Messina, M. Cannas, and R. Boscaino, Phys. Rev. B **83**, 174201 (2011).
[50]C. Zhang, J. Yang, Z. Quan, P. Yang, C. Li, Z. Hou, and J. Lin, Cryst. Growth Des. **9**, 2725 (2009).
[51]C. Zhang, C. Li, S. Huang, Z. Hou, Z. Cheng, P. Yang, C. Peng, and J. Lin, Biomaterials **31**, 3374 (2010).
[52]C. Wang, D. Liu, C. Zhang, J. Sun, W. Feng, X. J. Liang, S. Wang, and J. Zhang, ACS Appl. Mater. Interfaces **8**, 11262 (2016).
[53]R. K. Singh, T.-H. Kim, K. D. Patel, J.-J. Kim, and H.-W. Kim, J. Mater Chem. B **2**, 2039 (2014).
[54]S. Valizadeh, M. H. Rasoulifard, and M. S. S. Dorraji, Korean J. Chem. Eng. **33**, 481 (2016).
[55]S. Rehman, R. Ullah, A. M. Butt, and N. D. Gohar, J. Hazardous Mater. **170**, 560 (2009).
[56]T. Bak, J. Nowotny, M. Rekas, and C. C. Sorrell, Int. J. Hydrogen Energy **27**, 991 (2002).
[57]L. Cheng, M. D. Weir, H. H. Xu, J. M. Antonucci, N. J. Lin, S. Lin-Gibson, S. M. Xu, and X. Zhou, J. Biomed. Mater. Res. B Appl. Biomater. **100**, 1378 (2012).
[58]F. Nudelman, K. Pieterse, A. George, P. H. H. Bomans, H. Friedrich, L. J. Brylka, P. A. J. Hilbers, G. de With, and N. A. J. M. Sommerdijk, Nat. Mater. **9**, 1004 (2010).
[59]M. M. Kłosowski, R. Carzaniga, S. J. Shefelbine, A. E. Porter, and D. W. McComb, Sci. Rep. **8**, 3024 (2018).
[60]V. Uskoković, S. Marković, L. J. Veselinović, S. Škapin, N. Ignjatović, and D. P. Uskoković, Phys. Chem. Chem. Phys. **20**, 29221 (2018).
[61]A. Dey, P. H. Bomans, F. A. Müller, J. Will, P. M. Frederik, G. de With, and N. A. Sommerdijk, Nat. Mater. **9**, 1010 (2010).
[62]B. Xie, T. J. Halter, B. M. Borah, and G. H. Nancollas, Cryst. Growth Des. **14**, 1659 (2014).
[63]B. Wopenka and J. D. Pasteris, Mater. Sci. Eng. C **25**, 131 (2005).
[64]C. Rey, C. Combes, C. Drouet, and M. J. Glimcher, Osteoporos. Int. **20**, 1013 (2009).
[65]R. A. Harper and A. S. Posner, Proc. Soc. Exp. Biol. Med. **122**, 137 (1966).
[66]S. Jiang, H. Pan, Y. Chen, X. Xu, and R. Tang, Faraday Discuss. **179**, 451 (2015).
[67]V. Uskoković and T. A. Desai, J. Pharm. Sci. **103**, 567 (2014).
[68]S. Jiang, Y. Chen, H. Pan, Y. J. Zhan, and R. Tang, Phys. Chem. Chem. Phys. **15**, 12530 (2013).
[69]V. Uskoković, S. Tang, and V. M. Wu, ACS Appl. Mater. Interfaces **10**, 14491 (2018).
[70]H. Fleisch, Clin. Orthop. **32**, 170 (1964).
[71]E. D. Eanes and A. S. Posner, "Structure and chemistry of bone mineral," in *Biological Calcification Cellular and Molecular Aspects*, edited by H. Schraer (Appleton-Centyr Crofts, New York, NY, 1970), pp. 1–26.
[72]H. Cölfen, Nature **9**, 960 (2010).
[73]W. Li, J. Zhu, and Z. Mou, Petroleum Sci. **4**, 75 (2007).
[74]C. A. Orme and J. L. Giocondi, "The use of scanning probe microscopy to investigate crystal-fluid interfaces," in *Perspectives on Inorganic, Organic, and Biological Crystal Growth from Fundamentals to Applications*, edited by M. Skowronski, J. J. DeYoreo, and C. A. Wang (American Institute of Physics, Melville, NY, 2007).
[75]V. Uskoković, W. Li, and S. Habelitz, J. Bionic Eng. **8**, 114 (2011).
[76]A. Filankembo, S. Giorgio, I. Lisiecki, and M. P. Pileni, J. Phys. Chem. B **107**, 7492 (2003).
[77]L. Wang and W. Colon, Biochemistry **46**, 5562 (2007).
[78]V. Uskoković, Steroids **73**, 356 (2008).
[79]A. F. Gualtieri, Toxicol. Appl. Pharmacol. **361**, 89 (2018).
[80]C. Kinnear, T. L. Moore, L. Rodriguez-Lorenzo, B. Rothen-Rutishauser, and A. Petri-Fink, Chem. Rev. **117**, 11476 (2017).
[81]V. Uskoković, S. S. Batarni, J. Schweicher, A. King, and T. A. Desai, ACS Appl. Mater. Interfaces **5**, 2422 (2013).
[82]G. Bateson, *Mind and Nature: A Necessary Unity* (Hampton, Cresskill, NJ, 1979), p. 199.
[83]P. N. Lim, L. Chang, and E. S. Thian, Nanomed. Nanotechnol. Biol. Med. **11**, 1331 (2015).